KINETIC UNDERSTANDING OF THE SYNGAS-TO-DME REACTION SYSTEM AND ITS IMPLICATIONS TO PROCESS AND ECONOMICS

Topical Report

Prepared by
Xiang-Dong Peng

Contractor:

AIR PRODUCTS AND CHEMICALS, INC.
Allentown, PA 18195

December 2002

Prepared for the United States Department of Energy
Under Contract No. DE-FC22-94 PC93052

TABLE OF CONTENTS

ABSTRACT

In a single-step synthesis gas-to-dimethyl ether process, synthesis gas (or syngas, a mixture of H_2 and CO) is converted into dimethyl ether (DME) in a single reactor. The three reactions involved in this process, methanol synthesis, methanol dehydration and water gas shift, form an interesting reaction network. The interplay among these three reactions results in excellent syngas conversion or reactor productivity. A fundamental understanding of this interplay helps to explain many experimental and simulation observations, to identify optimal reaction conditions, and to provide guidelines for process development.

The higher syngas conversion or reactor productivity in the syngas-to-DME reaction system, compared to that in the syngas-to-methanol reaction system, is referred to as chemical synergy. This synergy exhibits a strong dependence on the composition of the reactor feed. To demonstrate the extent of this dependence, simulations with adjusted activity for each reaction were performed to reveal the relative rate of each reaction. The results show that the water gas shift reaction is the most rapid, being practically controlled by the equilibrium. Both methanol synthesis and methanol dehydration reactions are kinetically controlled. The kinetics of the dehydration reactions is greater than that of the methanol synthesis reaction in the CO-rich regime. However, the rates of these two reactions come closer as the H_2 concentration in the reactor feed increases.

The role of the dehydration reaction is to remove the equilibrium barrier for the methanol synthesis reaction. The role of the water gas shift reaction is more complex; it helps the kinetics of methanol dehydration by keeping the water concentration low, which in turn enhances methanol synthesis. It also readjusts the H_2:CO ratio in the reactor as the reactions proceed. In the CO-rich regime, the water gas shift reaction supplements the limiting reactant, H_2, by reacting water with CO. This enhances both the kinetics and thermodynamic driving force of the methanol synthesis reaction. In the H_2-rich regime, water gas shift consumes the limiting reactant, CO, which harms both the kinetics and thermodynamics of methanol synthesis. An understanding of these complex roles of the methanol dehydration and water gas shift reactions and of their dependence on the syngas composition explains why the synergy is high in the CO-rich regime, but decreases with increasing H_2 or CO_2 content in the reactor feed.

The methanol equivalent productivity of the syngas-to-DME reactor is also a strong function of the reactor feed. A mathematical approach was developed to understand this dependence. The approach divides a power law type of rate equation into two terms, the kinetic term (the rate of the forward reaction) and the thermodynamics or driving force term (1- approach to equilibrium). The equations for the best feed composition for each term were derived. The approach was developed for the single reaction system, and then extended to the syngas-to-DME reaction system. The equations provide insights into why and how the methanol synthesis in the syngas-to-DME system depends on the other two reactions. They can also be used to calculate the best feed composition for a given conversion. The analysis shows that for typical commercial syngas conversion, the optimal H_2:CO ratio for the LPDME™ reactor is around 1-to-1, in good agreement with the results from the simulation.

While the 1-to-1 feed provides a good foundation for some process configurations, it does not match the composition of natural gas-derived syngas, which typically has a H_2:CO ratio of 2:1 or greater. The process would also produce one CO_2 molecule for every DME product, both a materials utilization and an environmental problem. However, recycling CO_2 to the syngas generation unit can solve all of these problems. Integration schemes with different syngas generation technologies (dry reforming, steam methane reforming and partial oxidation) were developed. The feasibility of these schemes was illustrated by simulations using realistic kinetics, thermodynamics, and commercial conditions.

Finally, this report discusses the implications of the kinetic understanding and the resulting process schemes to the process economics. It was recognized that, for the overall process, the cost saving in the synthesis loop due to the reaction synergy is counteracted by the cost addition due to CO_2 formation and the resulting costly separation. This counteraction occurs in the entire H_2:CO range of commercial interest. The curves that showed the enhancement in productivity and CO_2 formation as a function of H_2:CO ratio in the reactor feed were used to discuss qualitatively how the economics of the syngas-to-DME process (1-step) compares to the syngas-to-methanol-plus-dehydration process (2-step). While the 1-step process has clear advantages over the 2-step process for CO-rich syngas derived from coal and other carbonaceous solids and liquids, its advantage for the natural gas-derived syngas is not so clear. Process optimization appears to be an important factor in tilting the balance.

1. Introduction

Over the past 15 years, Air Products & Chemicals, Inc., with U.S. Department of Energy (DOE) support, has been developing liquid phase technology to produce transportation fuels from synthesis gas (syngas) generated from coal and natural gas. Since the liquid phase operation (three phase slurry, bubble-column reactors) can accommodate the heat released from highly exothermic reactions, it is well suited to these applications. Liquid Phase Methanol (LPMEOH™) has been demonstrated on a large scale at Tennessee Eastman [1]. Liquid Phase Dimethyl Ether (LPDME™) is the next process in this progression [2,3]. Dimethyl ether (DME) has been identified as a potential diesel, cooking and power plant fuel [4-6], and can serve as a building block for liquid oxygenated compounds with high cetane numbers [7]. DME is also a potential chemical feedstock [8] and refrigerant replacement [9].

The main driving force for developing a single-step syngas-to-DME process is to produce DME at a cost lower than that from the commercially available two-step process, namely syngas-to methanol followed by methanol dehydration in sequential reactors. The cost penalties of the two-step process are (1) limited productivity in the syngas-to-methanol reactor due to equilibrium constraints, and (2) the need for a separate dehydration reactor and associated separation units.

The single-step syngas-to-DME process overcomes these two obstacles by combining the synthesis and dehydration reactions in a single reactor and utilizing the greater synthesis productivity made possible by a chemical synergy from the combined reactions.

Three reactions take place simultaneously in the syngas-to-DME reactor.

Methanol synthesis reaction:	$2H_2 + CO \Leftrightarrow CH_3OH$	(1)
Methanol dehydration reaction:	$2CH_3OH \Leftrightarrow CH_3OCH_3 + H_2O$	(2)
Water gas shift reaction:	$CO + H_2O \Leftrightarrow CO_2 + H_2$	(3)

Reactions (1) and (3) are catalyzed by a standard Cu-based methanol synthesis catalyst. Reaction (2) is catalyzed by a dehydration catalyst. The presence of the dehydration reaction frees the overall synthesis gas conversion from the equilibrium constraint imposed by the thermodynamics of methanol synthesis alone. The system offers further kinetic enhancement by lowering the water level through water gas shift reaction, therefore accelerating methanol dehydration. This synergy of methanol synthesis, methanol dehydration, and water gas shift gives higher syngas conversion per pass or productivity compared to the syngas-to-methanol process.

The synergy has long been recognized and demonstrated [10,11]. Experimental work has been conducted to study the performance of the reaction system as a function of various reaction parameters such as syngas composition (for example, H_2:CO ratio, CO_2 and H_2O content), catalyst materials and composition, space velocity, pressure, and temperature [2,12-15]. Noticeably absent from the prior work is a fundamental and systematic analysis of the reaction

system. Limited explanations have been attempted, but mostly on the basis of thermodynamics [10,14,16]. However, as we demonstrate below, the reaction system is far away from equilibrium at the typical industrial production conditions using commercially available catalyst materials. The synergy of the system is limited by the kinetics of the reaction system. Analysis based solely on thermodynamic equilibrium calculations is inadequate and could even be misleading. The inquiry into the mechanism of the synergy led us to a kinetic study of the reaction system. This, in turn, led to a better understanding of the process and economic aspects of the syngas-to-DME technology.

The first part of this report describes the kinetic understanding of this reaction system, including why the synergistic effect varies with reaction parameters; what kind of role each reaction plays in the synergy; and what the process guidelines are for optimizing the synergy. Identifying the kinetic conditions for the best productivity is of special interest, because it provides an opportunity to optimize the synergistic effect, making possible the production of DME at a cost lower than the two-step syngas-to-DME process.

How to accommodate the best kinetic conditions in a process is another practical matter. For example, our kinetic study demonstrates that the best overall reaction for the syngas-to-DME reactor is

$$3H_2 + 3CO \rightarrow CH_3OCH_3 + CO_2 \qquad (4)$$

While this gives the highest reactor productivity, it also sacrifices one third of the carbon to CO_2. In addition to low carbon utilization, generation of CO_2 is an environmental concern because CO_2 is a greenhouse gas. Furthermore, this reaction scheme poses a mismatch between the best syngas composition to the reactor (H_2:CO ratio of 1:1) and the composition of the syngas that can be generated by commercially available conversion units. The H_2:CO ratio from most syngas generation units is not 1:1, except for the case of the CO_2-methane reformer. For coal-derived, CO-rich syngas, this problem can be solved readily by injecting water into the reactor to provide the extra hydrogen through the water gas shift reaction. However, lowering the hydrogen content in natural gas-derived, H_2-rich syngas is not straightforward.

The second part of this report summarizes our efforts in developing process concepts and schemes to resolve the conflicts between establishing the best kinetic conditions for the reactor and the practical concerns of material utilization and availability. In brief, the problems are solved by integrating the DME reaction system with the syngas generation unit.

Kinetics or reactor productivity alone does not determine if the single-step process is more economical than the two-step process. In fact, the downstream separation in the single-step process is more complex, and possibly more costly, compared to the two-step process. This is due to CO_2 formation in the DME reactor (Reaction 2) and the difficulty associated with separating CO_2. The third part of this report discusses, qualitatively, how this CO_2 problem may affect the economics of the single-step process, mainly the trade-off between reactor productivity and CO_2 formation.

In summary, this report presents our understanding of three issues that are important in the development of the single-step syngas-to-DME process: reactor productivity, material utilization and availability, and separation difficulty. The report shows how these factors interplay and affect the economics of the process in a complicated manner. The report is not meant to be a firm evaluation of the economics of the single-step process. Such an evaluation would require detailed engineering study, and the conclusions would depend greatly on a specific type of process application, location, and situation.

All specific examples in this report, whether experimental or simulated, are based on a slurry phase reactor that behaves like a single, continuously stirred tank reactor (CSTR). Therefore, the results are directly applicable to the liquid phase syngas-to-DME process (LPDME™) under development at Air Products, which consists of a slurry phase autoclave or bubble column reactor with catalyst powders suspended in an inert liquid medium. However, the general understanding obtained from this study should also be valid for the gas phase syngas-to-DME process based on the packed-bed reactor, after the differences caused by a CSTR (slurry phase autoclave) versus a plug flow reactor (packed bed) are accounted for.

2. Details of Experiments and Simulations

All kinetic experiments were carried out in 300 cc slurry phase autoclave reactors. The dual-catalyst system consisted of a powdered mixture of a commercial, copper-based methanol synthesis catalyst and γ-alumina dehydration catalyst suspended in a hydrocarbon oil. For comparison, the results from liquid phase syngas-to-methanol (LPMEOH™) experiments were also used. In the LPMEOH™ experiments, the slurry contained only the methanol catalyst. The reactor behaved as a CSTR and was free of mass transfer limitations. Conditions used for all experiments were 250°C, 52 MPa, and an 80:20 weight ratio of the methanol synthesis catalyst to the methanol dehydration catalyst. The gas hourly space velocity of 6,000 sl/kg-hr was used in all kinetic simulations, unless otherwise specified.

The kinetic simulations were based on this lab reaction system, i.e., a CSTR and the same catalyst mixture. The reaction conditions were the same as described above. The rate expressions and constants for the three reactions were obtained using the standard reaction system. All three rate expressions were a power law form multiplied by an approach-to-equilibrium term as shown below:

Methanol synthesis reaction: $$R_m = k_m f_{H2}^{a1} f_{CO}^{b1} (1 - app._m) \quad (5)$$

Water gas shift reaction: $$R_w = k_w f_{CO}^{a2} f_{H2O}^{b2} / f_{CO2}^{c2} (1 - app._w) \quad (6)$$

Methanol dehydration reaction: $$R_d = k_d f_{MEOH}^{a3} / f_{H2O}^{b3} / f_{DME}^{c3} (1 - app._d) \quad (7)$$

where f_i stands for the fugacity of component i and *app.* is the approach to equilibrium. The methanol equivalent productivity (or MEP, defined as the methanol productivity plus two times the DME productivity) from various lab experiments and their corresponding simulations is

plotted in Figure 1. The good agreement indicates that the rate expressions and the process model can well serve the purpose of the current investigation.

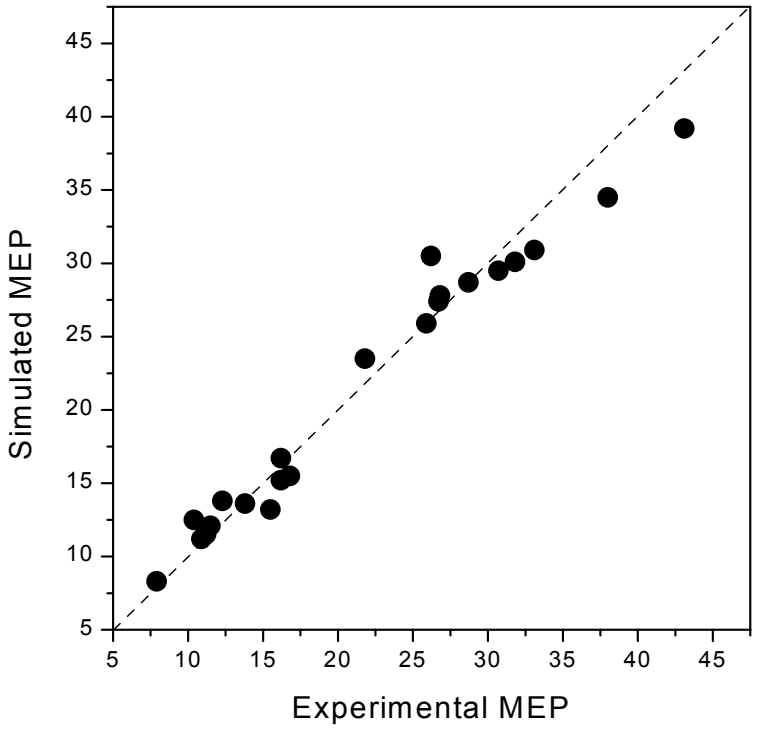

Figure 1: Comparison of the methanol equivalent productivity (MEP) from LPDME™ experiments with that from kinetic simulations.

Process simulations were used to demonstrate the technical feasibility of the process schemes described in this report. The syngas-to-DME reactor model was the same as that described above, except that the ratio of the methanol catalyst to the dehydration catalyst was changed from 80:20 to 50:50. For modeling the syngas generation unit, commercially relevant conditions were used. The CO_2 methane reformer and the steam methane reformer were simulated by thermodynamic equilibrium model. The methane partial oxidation reactor was modeled with a kinetic model that is based on our knowledge of the technology. The detailed information for each simulation is given when a specific process example is discussed. The separation units were simply specified to provide the desired separation; all separations can be achieved using commercially available technologies. A commercial process package, ASPEN PLUS, was employed in all simulations (both kinetics and process).

3. Kinetic Understanding

3.1. The Relative Rate of Each Reaction and Its Role in Chemical Synergy

The chemical synergy of the LPDME™ system is due to the interplay among methanol synthesis, methanol dehydration and water gas shift reactions. The synergy is reflected in the system's higher syngas conversion or productivity compared with methanol synthesis only (e.g., LPMEOH™). Therefore, one can use the percentage increase in the productivity from LPMEOH™ to LPDME™ under the same reaction conditions (i.e., temperature, pressure, space velocity, feed composition) as a quantitative measure of the synergy. Since one mole of DME is equivalent to two moles of methanol, one can use the MEP, defined as the methanol productivity plus two times the DME productivity, to compare the productivity of the two reaction systems. In this subsection, we will discuss the dependence of the synergy on the feed gas composition (e.g., H_2:CO ratio) and the underlying mechanism.

Columns 6 and 7 in Table 1 compare the MEP from LPDME™ experiments with that from the liquid phase methanol (LPMEOH™) experiments. These runs used the feed gases that simulate the syngas compositions of three typical industrial gasifiers, Shell, Texaco and Dow. LPDME™ gives much higher productivity than does LPMEOH™, clearly demonstrating the effect of the synergy.

Table 1: LPDME™ vs. LPMEOH™ for different feed gases.

Feed gas (mol%)	H_2	CO	CO_2	N_2	MEOH Equiv. Prod.*	
					LPMEOH	LPDME
Shell	30	66	3	1	16.4	29.4
Texaco	35	51	13	1	20.5	29.7
Dow	44	38	16	2	23.2	30

*: Mole of methanol equivalent per kilogram of total catalyst per hour.

However, the increase in MEP for LPDME™ differs for the three different types of syngas. The MEP nearly doubles in the Shell gas case, but increases by only 29% in the Dow gas case. In other words, there is more synergy in the Shell gas case than in the Dow gas case. This dependence on the syngas composition can be further illustrated by the simulations shown in Figure 2, which depicts the MEP for LPDME™ and LPMEOH™ as a function of H_2:CO ratio in the syngas feed. Not surprisingly, the synergy is observed in the entire range, as the MEP of LPDME™ is always greater than that of LPMEOH™. However, the magnitude of the synergy varies with H_2:CO ratio. For a H_2:CO above 1.5, the percentage increase in MEP is around 20%. This increase becomes 45% at a H_2:CO of 1.0 and 90% at a H_2:CO of 0.5. In other words, the greater the proportion of CO, the greater the chemical synergy.

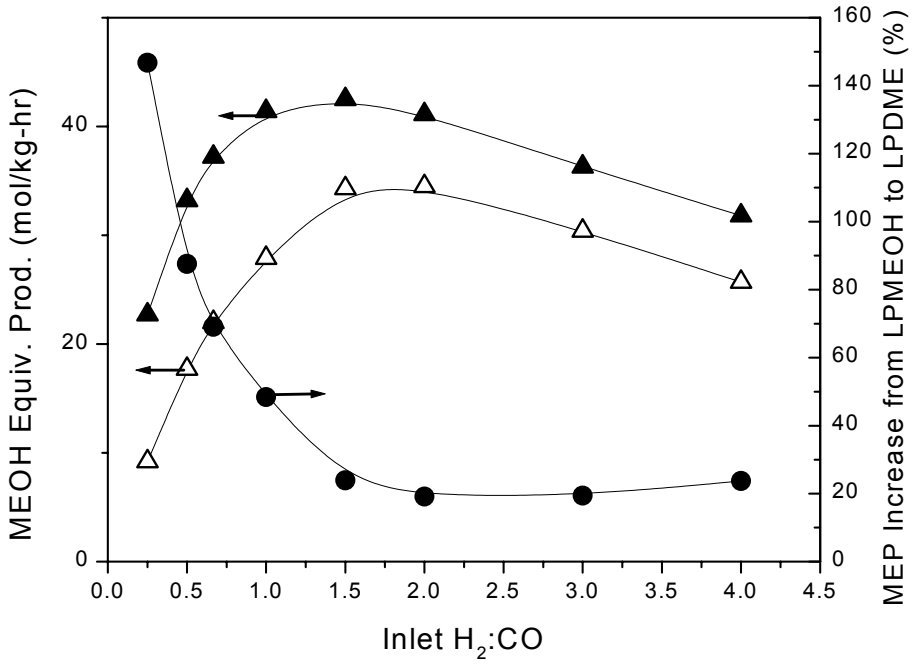

Figure 2: The methanol equivalent productivity from LPDME™ (▲), the methanol productivity from LPMEOH™ (Δ), and the percentage increase in the methanol equivalent productivity from LPMEOH™ to LPDME™ (●) as a function of H_2:CO ratio in the syngas feed.

To understand the dependence of the chemical synergy on the H_2:CO ratio of the reactor feed, let us first determine if the reaction system is limited by thermodynamics or kinetics. If it is the latter, then what is the rate-determining reaction(s) in the system? This can be ascertained by simulating the change in MEP while varying the rate constant for each reaction. Figure 3 depicts the MEP for (1) our base catalyst system (k_m, k_d and k_w), (2) the system with the methanol synthesis activity increased by a factor of 4 ($4k_m$, k_d and k_w), (3) the system with the dehydration activity increased by a factor of 4 (k_m, $4k_d$ and k_w), and (4) the system with the water gas shift activity increased by a factor of 4 (k_m, k_d and $4k_w$). Also shown in the figure is the MEP when the system is at thermodynamic equilibrium.

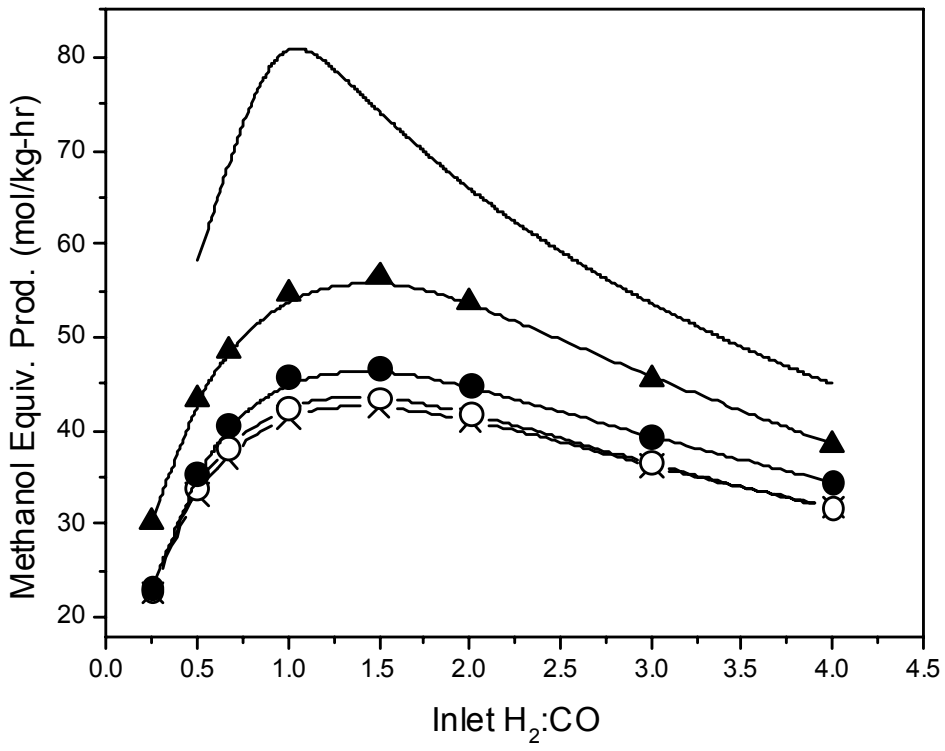

Figure 3: The methanol equivalent productivity as a function of H_2:CO ratio in the syngas feed for catalyst systems with different activities. (x) k_m, k_d and k_w, i.e., the base catalyst system; (●) k_m, $4k_d$ and k_w; (▲) $4k_m$, k_d and k_w; (o) k_m, k_d and $4k_w$; (—) at equilibrium.

An examination of Figure 3 leads to four observations. First, the reaction system is kinetically limited. At the maximum productivity (H_2:CO of about 1:1), the MEP with the base catalyst system (k_m, k_d and k_w) is only one half of the potential maximum MEP. This observation holds true even when a space velocity as low as 2000 is used (not shown). Therefore, to understand the reaction system, one needs to look at the kinetics. Using only thermodynamic equilibrium calculations is inadequate and possibly misleading.

Second, the rate of the water gas shift reaction is much greater than the rate of the other two reactions. Quadrupling the rate constant of the shift reaction (case of k_m, k_d and $4k_w$) results in little increase in MEP. The simulations also show that the water gas shift reaction is essentially thermodynamically limited in the entire range of this study.[1] Therefore, the role of this reaction in the synergy is to re-adjust the concentration of H_2, CO, CO_2, and H_2O through the thermodynamic equilibrium among the four components. This could have positive or negative effects on the synergy, as will be shown below.

Third, both methanol synthesis and methanol dehydration reactions are kinetically limited. Increasing the rate constant of each of these two reactions results in higher MEP. These two reactions are not limited by thermodynamic equilibrium because the products from each are

consumed by other reactions. For methanol synthesis, the methanol produced is consumed by the dehydration reaction. For methanol dehydration, the water produced is shifted by the water gas shift reaction. Since methanol dehydration and water shift to hydrogen are in sequence, one can view the fast water gas shift reaction as the ultimate sink to drive the system away from equilibrium limitations. In this regard, the water gas shift reaction always has a positive effect on the synergy.

Fourth, Figure 3 demonstrates that increasing the methanol synthesis rate constant (k_m) produces a greater increase in MEP than increasing the dehydration rate constant (k_d). This indicates that methanol synthesis is more rate determining than methanol dehydration with our base catalyst system. This is completely true in the CO-rich end of the result, since increasing the dehydration rate constant has little effect on MEP. As the H_2:CO ratio in the reactor feed increases, increasing dehydration activity starts to show positive effects on MEP. This suggests that the kinetics of the two reactions become more comparable to each other as the reactor feed becomes less CO-rich.

In summary, Figure 3 shows that the LPDME™ reaction system is kinetically limited. The kinetics of the water gas shift reaction is much greater than that of the other two reactions. In terms of its effects on the other two reactions, the water gas shift reaction is essentially thermodynamically limited. This fast reaction provides the ultimate sink to drive the other two reactions away from equilibrium. It also re-adjusts the concentration of H_2, CO, CO_2, and H_2O as the reactions proceed. The kinetics of methanol synthesis is slower than that of methanol dehydration. Therefore, methanol synthesis is a more rate-determining step between the two kinetically controlled reactions. However, this difference becomes smaller as the H_2:CO ratio in the reactor feed increases.

This general picture can help us to understand why the synergy depends on the composition of the reactor feed. Figure 2 shows that there are three regimes in which the synergetic effect differs greatly. In the CO-rich regime (H_2:CO <0.75), the synergy is large (>60%) and increases rapidly with decreasing H_2:CO ratio. In contrast, the synergy is small (around 20%) in the H_2-rich regime (H_2:CO >2) and insensitive to the H_2:CO ratio. There is also an intermediate regime (0.75<H_2:CO <2) in which the synergy levels off from 60 to 20%. These differences are due to the interplay among the three reactions in the LPDME™ system. They also depend on how methanol synthesis alone (e.g., LPMEOH™) is affected by the feed gas composition.

In the CO-rich regime, the productivity for methanol synthesis alone is low (see the LPMEOH™ curve in Figure 2). This occurs because the H_2 content in the reactor feed is very low compared to that required by the reaction (H_2:CO =2), and H_2 is quickly depleted as the reaction proceeds. Not only does this affect methanol synthesis due to the poor availability of one of its reactants, it also quickly brings the system to equilibrium. (Note that the approach to methanol synthesis equilibrium is defined by $f_{me}/(\mathbf{f_{H2}})^2/f_{CO}/K_m$, where *f* stands for fugacity.)

In the LPDME™ system, both problems are mitigated by the dehydration and water gas shift reactions. The dehydration reaction removes its methanol product, expanding the equilibrium boundary. Most of the water formed in the dehydration reaction is converted into H_2. This self-generated H_2 supply enhances methanol synthesis by replenishing the much-needed limiting

reactant and slowing down the approach to equilibrium. In other words, the methanol dehydration and water gas shift reaction have three positive effects on methanol synthesis in the CO-rich regime: (1) consuming methanol to expand the equilibrium boundary, (2) forming H_2 to replenish the limiting reactant, and (3) forming H_2 to slow down the equilibrium. The CO-rich atmosphere enables these three effects to reach their fullest extent. The water gas shift equilibrium drives almost all water into H_2 because the atmosphere is CO-rich. The dehydration kinetics are much greater than the methanol synthesis kinetics, partly because the lack of H_2 slows methanol synthesis, and partly because the dehydration reaction is not hindered by water (see below). The faster dehydration kinetics keeps the methanol concentration low. Therefore, the equilibrium barrier for methanol synthesis is minimal. All of these explain why the greatest synergy is observed in the CO-rich regime.

These arguments are illustrated by the simulated results shown in Figures 4 and 5. Figure 4 depicts the exit composition as a function of reaction feed composition for the base catalyst system. Indeed, the water and methanol concentration is low in the CO-rich regime. Figure 5 shows the approach to methanol synthesis equilibrium for both LPMEOH™ and LPDME™. A greater decrease in the approach is observed in the CO-rich regime from LPMEOH™ to LPDME™.

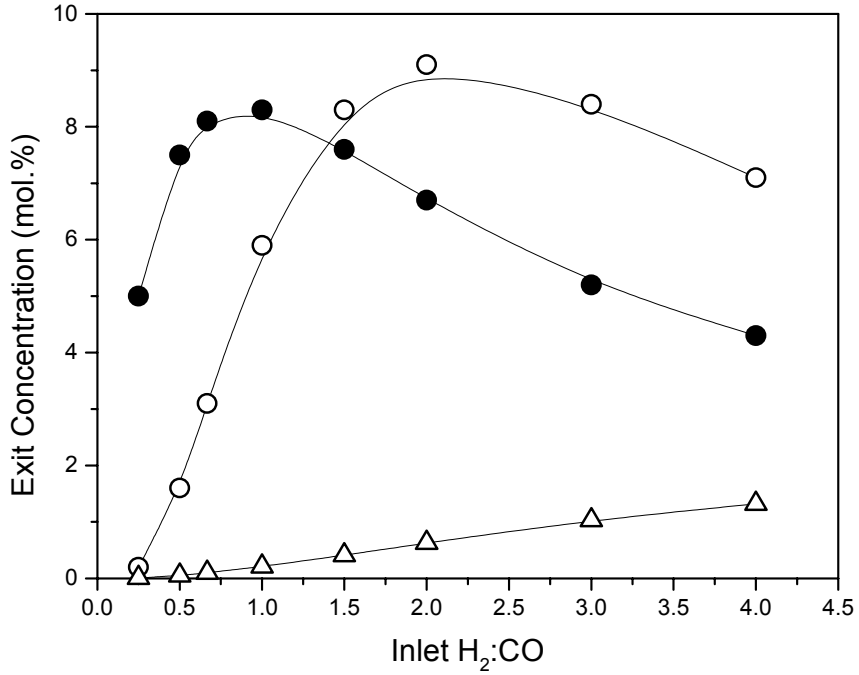

Figure 4: The exit concentration of methanol (O), DME (•) and water (Δ) as a function of H_2:CO ratio in the syngas feed for the base catalyst system. All catalyst activities are in their base values.

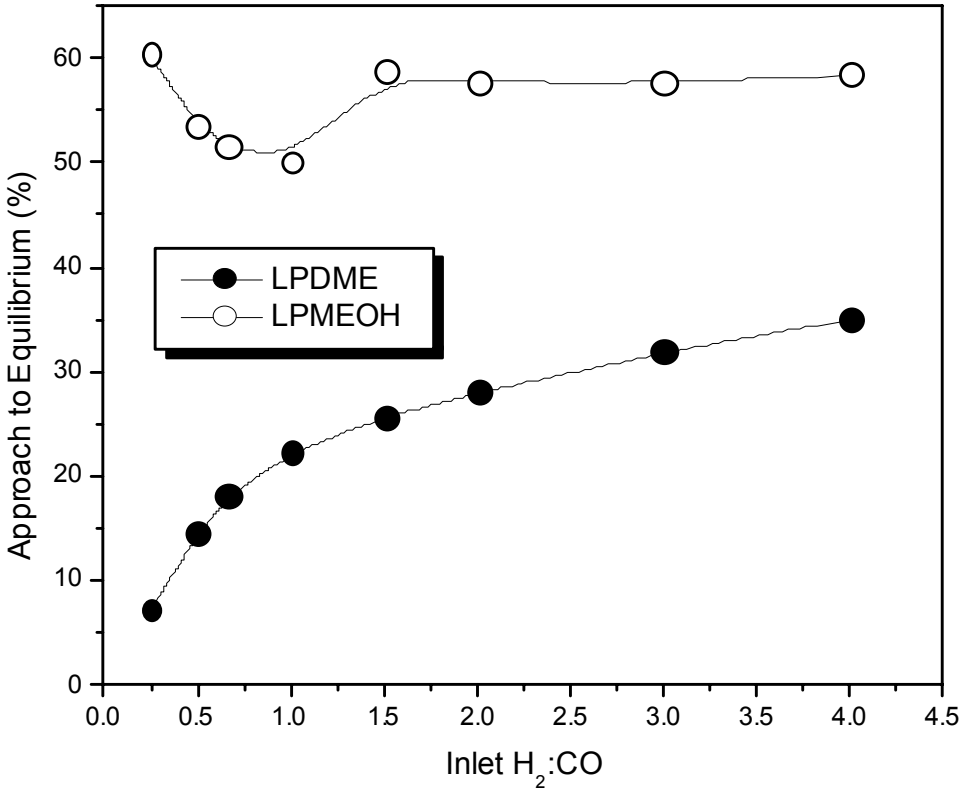

Figure 5: The approach to methanol synthesis equilibrium for LPMEOH™ (o) and LPDME™ (•) as a function of H_2:CO ratio in the reactor feed.

In the intermediate regime (0.75 <H_2:CO <2), all three positive effects of the methanol dehydration and water gas shift reactions still contribute to the synergy, but to a lesser extent. First, the kinetics of methanol synthesis improves as the H_2:CO ratio increases. The lack of H_2 is no longer sharply felt as in the CO-rich regime. Therefore, replenishing H_2 through the water gas shift reaction has less effect on methanol synthesis.

Second, the dehydration kinetics is less effective at removing methanol, and therefore it is less effective at expanding the equilibrium boundary for methanol synthesis. The kinetics of methanol dehydration no longer dominates that of the methanol synthesis reaction, as evidenced by the increasing methanol concentration in this regime (Figure 4). This occurs partly because the kinetics for methanol synthesis is greater due to better H_2 availability, and partly because the dehydration reaction is retarded by the increasing amount of one of its products, water, in this regime (Figure 4). This self-restricting behavior for the methanol dehydration reaction has long been known [17] and is reflected in our kinetic model (Equation 7). This retardation is evidenced by the results shown in Figure 4. Although the methanol concentration increases as the H_2:CO ratio increases (higher reactant concentration for dehydration), the DME concentration decreases (lower dehydration rate), accompanied by increasing water concentration. The lower dehydration rate is totally due to the water retardation, because the

approach to methanol dehydration equilibrium is around 1% in the regime. The increasing water concentration with increasing H_2:CO ratio is determined by the water gas shift equilibrium. In brief, the decreasing synergy in this regime is due to the diminishing positive effects by the water gas shift and methanol dehydration reactions as the H_2:CO ratio increases.

Now let us explain why there is little synergy in the H_2-rich regime (H_2:CO>2). With an even higher H_2:CO ratio, the effect of the methanol dehydration reaction on expanding the methanol equilibrium boundary becomes even smaller. What further diminishes the synergy is the role change of the water gas shift reaction. Note that the limiting reactant for methanol synthesis becomes CO in this regime. Shifting the water formed by dehydration depletes CO, reducing the availability of the limiting reactant for methanol synthesis. It also accelerates the approach to methanol synthesis equilibrium (the approach = $f_{me}/(f_{H2})^2/\mathbf{f_{CO}}/K_m$). Therefore, the two positive effects of the water gas shift reaction in the other two regimes become negative in the H_2-rich regime. With the negative effects of the water gas shift reaction and smaller positive effect of the dehydration reaction, the synergy decreases.

Although these observations were made from a reactor feed containing only H_2 and CO, the understanding gained can be applied to more general cases. For example, the above discussion shows that as H_2:CO in reactor feed increases, the three positive effects of methanol dehydration and water gas shift reactions decrease. This is due to the less favorable equilibrium conditions for water conversion into hydrogen. It follows then that increasing the CO_2 content in the reactor feed should have a similar effect (cf., Equation 3). This is borne out by the simulation shown in Figure 6: MEP decreases with increasing CO_2 concentration in the syngas feed, accompanied by an increase in the water concentration. This agrees well with the experimental observation that removing CO_2 in the syngas feed leads to higher productivity [2]. CO_2 is an undesirable component in the feed because, like H_2, it adversely affects the synergy by building up water, but unlike H_2, CO_2 does not contribute to methanol synthesis under syngas-to-DME conditions.

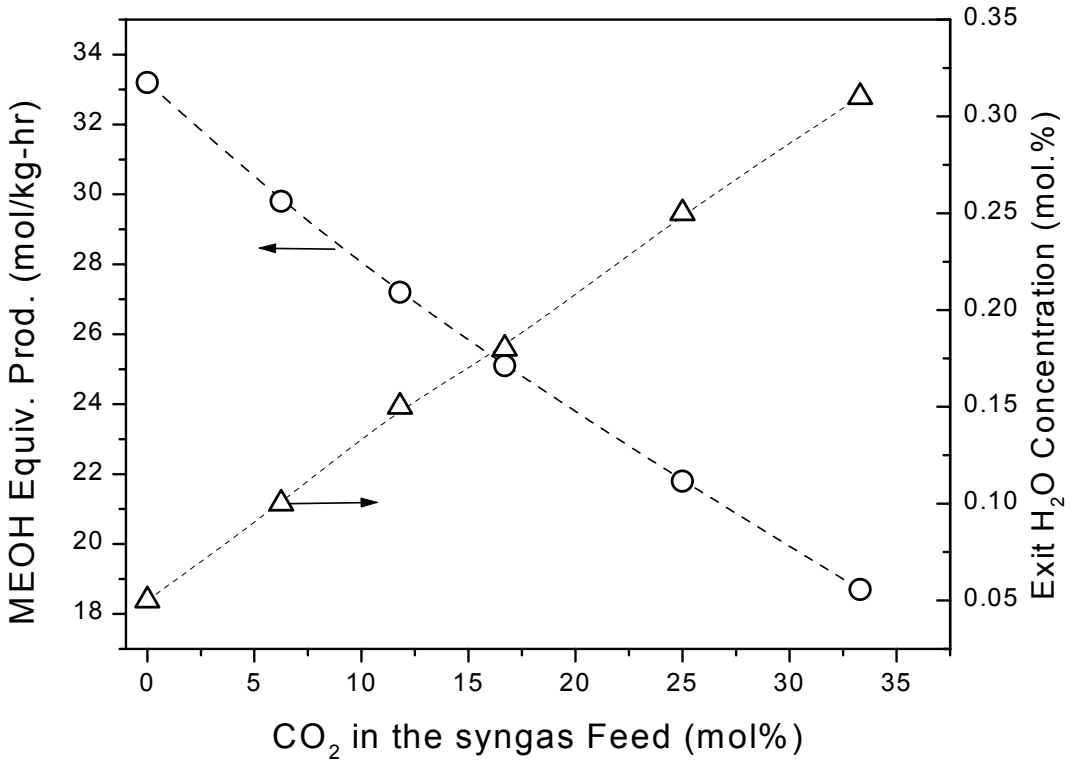

Figure 6: The methanol equivalent productivity and the exit water concentration as a function of CO_2 concentration in the syngas feed. H_2:CO ratio is fixed at 1:2.

We can now explain the question asked at the beginning of this section: Why were different synergetic effects observed in our lab experiments using three different types of syngas (Table 1)? The feed gas in all these cases no longer contains only H_2 and CO, but also CO_2. However, the collective effect of these three gases on the synergy can be explained in terms of the $[H_2]*[CO_2]/[CO]$ ratio in the feed. Since the water gas shift reaction is practically equilibrium limited, the water level (not measured in these experiments) should be somehow proportional to this ratio. Then, as expected, the increase in MEP from LPMEOH™ to LPDME™ decreases with an increase in this ratio, accompanied by an increase in the experimentally measured methanol concentration (Figure 7).

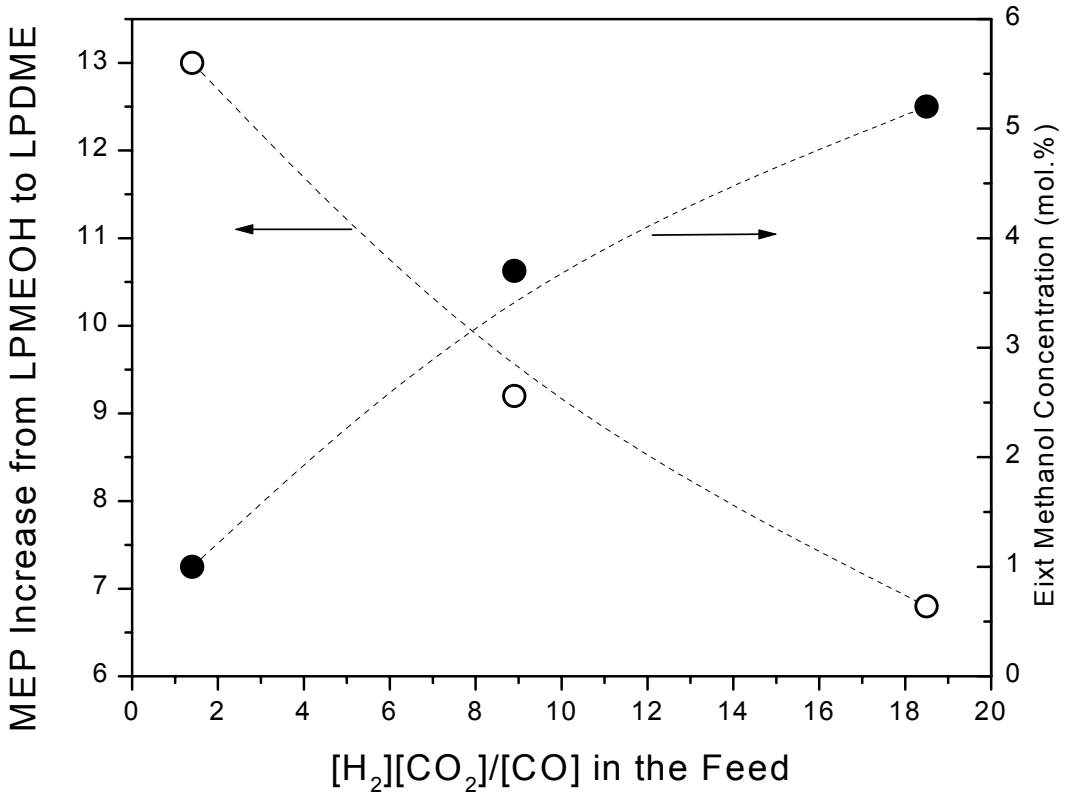

Figure 7: The MEP increase from LPMEOH™ to LPDME™ and the exit methanol concentration as a function of the $[H_2][CO_2]/[CO]$ ratio in the syngas feed.

The results discussed above have the following process and commercial implications.

(1) There is considerable synergy under CO-rich conditions. Therefore, for a fixed CO-rich reactor feed (e.g., coal-derived syngas in a once-through operation), the syngas-to-DME process will give a much higher MEP than the syngas-to-methanol process. In practical process engineering terms, this means that there is a potential for greater operating flexibility in an electricity-chemical co-production arrangement with IGCC.

(2) It is preferred that CO_2 in the feed be minimized.

(3) The DME system is far from reaching its thermodynamic equilibrium limitations. If the reaction rates could be increased by development of more active catalysts, syngas-to-DME would be a very attractive process for syngas conversion.

3.2. The Best Feed Gas Composition for the LPDME™ Process

While the previous subsection focuses on the mechanism of the chemical synergy, i.e., comparison between LPDME™ and LPMEOH™, this subsection concentrates on the best

reactor feed composition for the LPDME™ process and the underlying mechanism. As shown in Figure 2, although the chemical synergy in syngas-to-DME is better utilized under CO-rich conditions, the maximum MEP is obtained between H_2:CO ratios of 1:1 and 2:1, not at the CO-rich end. This can be ascribed to the trade-off between the best syngas composition for methanol synthesis and that for the synergy, since methanol synthesis is favored by a H_2-rich environment with the maximum rate at a H_2:CO ratio of 2:1 (see the LPMEOH™ curve in Figure 2). A detailed mathematical analysis of this trade-off is given in this subsection. We will first develop an approach for analyzing the best reactor feed for a single reaction system. The LPMEOH™ system will be used to illustrate this approach. Then the approach will be extended to analyze the best feed for LPDME™, a more complex, multi-reaction system.

3.2.1. A General Approach for Analysis of the Best Reactor Feed - Two-Term Approach

The rate expression of reversible reactions, in general, can be expressed as

$$R = \Phi(p_i, k_j, K_l)(1 - appr.) \tag{8}$$

where *appr.* is the approach to reaction equilibrium, defined as

$$appr. = \prod p_i^{vi} / K \tag{9}$$

In Equations 8 and 9, p_i is the partial pressure of Species *i*; k_j and K_l in Equation 8 are the rate constants and adsorption equilibrium constants, respectively; and υ_i and *K* in Equation 9 are the reaction stoichiometric coefficient of Species *i* and the reaction equilibrium constant, respectively. The important step in the current approach is to break down this rate expression into two terms.

The first term is $\Phi(p_i, k_j, K_l)$. The physical meaning of this term is the rate of forward reaction, or *RFR*. When *appr.* is zero and the reaction is completely controlled by the kinetics, the reaction rate equals *RFR*. Therefore, we call this term the "kinetic component of the reaction rate." The specific form of *RFR* varies from one system to another. Among the simple forms is the power law expression. For the Langmuir-Hinshelwood type of models for heterogeneously catalyzed reactions, *RFR* is generally a function of the partial pressures of the reactants to certain powers, divided by some dependence on the adsorption of reactants and/or products on the catalyst.

The second term, *(1-appr.),* is the thermodynamic driving force of the reaction. When *appr.* equals one, i.e., the reaction is at equilibrium, the reaction rate is zero. We call this term the "thermodynamic component of the rate expression" and denote it as *TDF* (Thermodynamic Driving Force).

With these definitions Equation 8 becomes

$$R = RFR \cdot TDF \tag{10}$$

We decompose the reaction rate into the two terms for the following reasons. As shown later, these two terms are essential components of the reaction rate, governed by two different mechanisms. RFR is defined by the kinetics of the reaction and TDF by the reaction stoichiometry or thermodynamics. Since the dependence of these two terms on the feed composition is usually different, analysis of the best feed composition for the reaction rate, the combined form of the two components, is often seemingly ill defined and case specific, in addition to possessing a mathematical complexity that makes analytical solutions difficult. When the rate is decomposed into its essential components, general analysis can be conducted for each component. Combining these individual understandings would allow one to understand the effect of the feed composition on the overall rate of the reaction. The simpler mathematics involved also facilitates the analytical solutions.

This approach also has practical implications. When the reaction is kinetically controlled (irreversible, large equilibrium constant or small conversion) or thermodynamically controlled (small equilibrium constant or large conversion), the understanding and results developed from the individual analysis can be applied directly.

Since our goal is to minimize the size of a reactor for a given productivity or maximize reactor productivity for a given reactor size, a reactor model is needed for the analysis. For mathematical simplicity, we chose the well-mixed reactor under steady-state operating conditions. With this selection, the volumetric space-time yield of a desired product i, F_i, becomes

$$\frac{F_i}{V} = R = RFR \cdot TDF \tag{11}$$

where V is the reactor volume. Equation 11 shows that for this reactor type, optimizing the space-time yield or minimizing reactor volume becomes exactly the same as optimizing the reaction rate. Furthermore, one needs to deal with only two compositions, the feed and effluent compositions, with the latter being the same as the composition throughout the reactor.

One can determine the best feed composition for the kinetic component of the reaction rate by solving

$$\frac{\partial RFR}{\partial x}\Big|_{\xi} = 0 \tag{12}$$

In Equation 12, x is the parameter that defines the feed gas composition, and ξ is the extent of the reaction. One of the physical meanings of Equation 9 is as follows. If the reaction is determined

by the kinetics, as in *appr.* << 1 and $F_i/V \approx RFR$ (cf. Equation 8), the feed composition derived from Equation 12 will give the smallest reactor size for a given ξ. This is equivalent to maximizing product yield (or total conversion) for a given reactor volume, since F_i is proportional to ξ, and ∂ξ/∂x is set to zero in solving Equation 12.

Likewise, the best feed for the thermodynamic term of the reaction rate can be obtained by solving

$$\left.\frac{\partial TDF}{\partial x}\right|_{\xi} = -\left.\frac{\partial (appr.)}{\partial x}\right|_{\xi} = 0 \qquad (13)$$

The physical meaning of Equation 13 is that for a given ξ, the feed composition derived from Equation 13 will give the greatest driving force, and therefore, the largest contribution from the thermodynamic term to the reaction rate. Note that TDF is bounded by 1 (at the onset of the reaction) and 0 (at reaction equilibrium). The greatest driving force means that the distance between the given ξ and the extent of the reaction at equilibrium, ξ^*, is the greatest for the feed composition derived from Equation 13. In other words, the best feed composition gives the greatest ξ^*, and solving Equation 13 is equivalent to finding the feed that gives maximum equilibrium productivity or total conversion. Therefore, an alternative way to find the best feed composition for TDF is to solve

$$\frac{d\xi^*}{dx} = 0 \qquad (14)$$

using the equilibrium equation. Equations 13 and 14 are mathematically equivalent. Equation 14 clearly shows that the best feed composition for TDF is a thermodynamic property of the reaction, independent of process parameters such as the extent of reaction, reactor volume, and the type of reactor.

3.2.2. Illustration of the Approach Using a Single Reaction System with Power-Law Rate Expression

This section illustrates the approach using a general, single-reaction system

$$aA + bB \Leftrightarrow rR + sS \qquad (15)$$

with a power-law rate expression

$$R = kp_A^{\alpha} p_B^{\beta} (1 - appr.) \qquad (16)$$

The reactor feed and effluent compositions for this reaction are:

	A	B	R	S	Total	
Feed:	$N_A^o = (1-x)N^o$	$N_B^o = xN^o$	N_R^o	N_S^o	$N^o+N_R^o+N_S^o$	(17)
Effluent:	$(1-x)N^o - a\xi$	$xN^o - b\xi$	$N_R^o + r\xi$	$N_S^o + s\xi$	$N^o+N_R^o+ N_S^o-(a+b-r-s)\xi$	(18)

All quantities in mass balance Equations 17 and 18 are in moles. The ξ stands for the extent of reaction, and *x* is the variable we will optimize against to find the best reactor feed. Note that *x* is no longer the molar fraction of reactant B in the reactor feed if the feed contains product species ($N_R^o \neq 0$, $N_s^o \neq 0$) and/or inerts (not shown). It relates to the ratio of the two reactants by x=1/(1+R), where R= N_A^0 / N_B^0.

The Best Feed for the Thermodynamics

For a single reaction system, a general equation of the best feed for the thermodynamic component of the reaction rate can be derived from Equation 13, since appr. has a general form as shown in Equation 9. For the reaction defined by Equation 15,

$$appr. = \frac{p_R^r p_S^s}{K p_A^a p_B^b} \tag{19}$$

Solving Equation 13 along with Equation 19, one obtains

$$\left(\frac{p_A}{p_B}\right)_{best} = BR = \frac{a}{b} \tag{20}$$

where *BR* stands for the best ratio of the reactants in the reactor or under reaction conditions for TDF. Equation 20 indicates that when BR agrees with the reaction stoichiometry, the reaction has the best TDF. Combining Equation 20 with Mass Balance Equation 18 gives

$$\left(\frac{N_A^0}{N_B^0}\right)_{best} = \frac{1-x}{x} = \frac{a}{b} \tag{21}$$

Equation 21 shows that the best feed for the thermodynamic component of the reaction rate is that which agrees with the reaction stoichiometry. This kind of feed is generally known as "stoichiometric" or "balanced" feed. It is common knowledge that the stoichiometric feed gives the best overall conversion, or materials utilization. The above analysis shows that it also gives the best thermodynamic driving force for the reaction. Note that Equation 21 is not a function of

the extent of reaction (ξ). This means that this ratio is solely determined by the reaction stoichiometry. It remains constant as the reaction progresses and the best driving force condition in the reactor defined by Equation 20 is always satisfied. For practical concerns, this implies that the best feed composition for the thermodynamic part of the reaction rate is independent of process parameters such as residence time or reactor volume. Therefore, the observation applies to any type of reactor.

The Best Feed for the Kinetics

Unlike the thermodynamic part of the problem discussed above, there is not a general form for RFR; it varies from one reaction system to another. Even for a given reaction, the form of RFR can be different, depending on how it is derived and what mathematical form one selects to represent the kinetics. For illustrative purposes, we will use a RFR with the following power-law form (cf., Equation 16)

$$RFR = kp_A^{\alpha} p_B^{\beta} \tag{22}$$

Solving Equation 12 along with Equation 22, one obtains

$$\left(\frac{p_A}{p_B}\right)_{best} = BR = \frac{\alpha}{\beta} \tag{23}$$

Equation 23 indicates that when the ratio of the two reactants in the well-mixed reactor is the same as the ratio of the orders of the reaction with respect to each reactant, one has the greatest RFR for a given extent of reaction. *BR* in Equation 23 stands for the best ratio of reactants for RFR in the reactor. Substituting mass balance Equation 18 into Equation 23, one obtains

$$\left(\frac{N_A^0}{N_B^0}\right)_{best} = \frac{\alpha}{\beta}\left(\frac{1-(\frac{b}{a}-\frac{\beta}{\alpha})a\xi/N^0}{1+(\frac{\alpha}{\beta}-\frac{a}{b})b\xi/N^0}\right) \tag{24}$$

Equation 24 gives the best feed composition for the kinetic component of the reaction rate.

To understand the physical meaning of Equation 24, we will define another two concepts. The first one is *Deviation,*

$$Deviation = \frac{\alpha}{\beta} - \frac{a}{b} \tag{25}$$

And the second one is *Feed Adjustment*,

$$FA = \left(\frac{1 - (\frac{b}{a} - \frac{\beta}{\alpha}) a\xi / N^0}{1 + (\frac{\alpha}{\beta} - \frac{a}{b}) b\xi / N^0} \right) \tag{26}$$

When *Deviation* is zero ($\alpha/\beta = a/b$), we say that the kinetics of the reaction (RFR) agree with the reaction stoichiometry. In this case, $FA = 1$ and $(N_A^0 / N_B^0)_{\text{best}}$ is independent of the extent of reaction (ξ). That is, one can start the reaction with the ratio of the two reactants at α/β, and this ratio remains unchanged as the reaction progresses. For any given extent of reaction, the BR defined by Equation 23 is always satisfied. In contrast, when *Deviation* is not zero ($\alpha/\beta \neq a/b$), or when the kinetics of the reaction (RFR) deviate from the reaction stoichiometry, $(N_A^0 / N_B^0)_{\text{best}}$ depends on the extent of reaction. That is, if one wants the best ratio of the two reactants in the reactor as defined by Equation 23 for a given extent of reaction (ξ), the ratio in the reactor feed needs to be adjusted away from α/β by a factor of *FA*.

The Best Feed for the Reaction

Equation 21 and Equation 24 define the bounds of the best feed composition for the overall rate of the reaction. For this simple reaction system with a simple power-law rate expression, a simple equation of the best ratio of reactants for the overall reaction can be derived by solving

$$\frac{\partial R}{\partial x}\Big|_{\xi} = 0 \tag{27}$$

This gives

$$\left(\frac{p_A}{p_B} \right)_{best} = BR = \frac{\alpha(1 - appr.) + a \cdot appr}{\beta(1 - appr.) + b \cdot appr.} \tag{28}$$

Equation 28 clearly shows that RFR and TDF are two essential components of the reaction rate. This equation reduces to Equation 23 at a low approach to equilibrium (BR for the kinetic component of the reaction rate). For a high approach to equilibrium, it approaches Equation 20 (BR for the thermodynamic component of the reaction rate). For the intermediate region, the best ratio for the overall reaction can be calculated from Equation 28 once ξ (a design parameter) is given. The best feed composition for the overall reaction can then be obtained using mass balance Equation 18.

General Applicability

Although the derivation in the last section is based on the reaction defined by Equation 15, the results are not limited by the specific form of the reaction, namely, the number of the reactants and products in the reaction. This is rigorously true for the results from the TDF part of the analysis. First, the partial pressures of products are a function only of the extent of reaction, independent of reactor feed composition. They will drop out during optimization. Therefore, the number of products in a single reaction system is not a factor in optimization. For a single reaction system containing more than two reactants, it can readily be shown that under the reaction conditions for TDF, the best ratio of any pair of reactants, reactants *i* and *j,* is υ_i / υ_j. The same is true for the ratio of reactants *i* and *j* in the best reactor feed. This means that the best feed composition for TDF is the composition defined by the reaction stoichiometry. Therefore, the observation on the best feed composition for TDF from the above analysis can be applied, in general, to any single reaction system. That is, the stoichiometric or balanced feed gives the maximal thermodynamic driving force to the reaction, independent of the extent of reaction. This observation may not apply to multi-reaction systems, as shown below. Physically, the optimization depends upon the logistically best supply of reactants to the reaction. The stoichiometric feed prevents any one reactant from becoming the limiting reagent or prevents the reaction system from approaching equilibrium prematurely as a result of short supply of one of the reactants.

The results from the RFR part of the analysis in the last section are based on (1) a power-law form RFR and (2) a single reaction system containing two reactants. However, the results are not limited by Condition 1. First, the concept BR itself is general for any single reactions, regardless of the mathematical representation of their kinetics. Physically, there is always a ratio of the reactants under the reaction conditions that gives the maximal RFR for the reaction. Using Equation 12 this ratio can be calculated, analytically or numerically, for any mathematical representations of RFR. Or BR can simply be obtained by experimental measurements, such as measuring the reaction rate as a function of feed composition at low conversion. Once BR is known, Deviation and FA can be calculated by Equations 25 and 28, respectively. Note that only mass balance is involved in going from Equation 20 to Equations 25 and 28. Therefore, these two equations are applicable to any single reaction systems, regardless of the form of the rate expression. The only modification necessary is to replace α/β with BR in these two equations.

For a single reaction containing more than two reactants, BR, Deviation and FA can still be used to define the problem. If the optimization is between two of the reactants, the results shown by Equations 23, 25 and 26 remain valid. However, if the optimization is among all of the reactants, the mathematics will be different, and the specific results shown in these equations will not be applicable.

3.2.3. Applications to Syngas-to-Methanol Reaction System

Syngas-to-Methanol Reaction System <u>without</u> Water Gas Shift Reaction

The syngas-to-methanol reaction system is described by Equation 1. In general, this reaction is accompanied by the water gas shift reaction (Equation 3) because commercially used, copper-based methanol synthesis catalysts also possess water gas shift activity. However, if the feed gas does not contain a significant amount of CO_2 and/or water, the water gas shift reaction is negligible, and one can consider this a single reaction system, similar to the general case discussed above. Therefore, the results in the last section can be directly applied. From Equation 21, we know that the best feed composition for the thermodynamic component of the reaction rate (TDF) is

$$\left(\frac{N_{H2}^0}{N_{CO}^0}\right)_{best} = \frac{a}{b} = 2 \tag{29}$$

That is, a H_2:CO ratio of 2 in the feed syngas will provide the best thermodynamic driving force for the reaction. For the kinetic part (RFR), let us use the power law rate expression we have used in our lab work, as described in Section 2,

$$R_m = k_m p_{H2}^{\alpha} p_{CO}^{\beta} (1 - \frac{p_{CH3OH}}{K_m p_{H2}^2 P_{CO}}) \tag{30}$$

where Subscript *m* stands for the methanol synthesis reaction. Ratio α/β in this empirical kinetic model happens to be to 2. Therefore, the Deviation of the kinetics from the reaction stoichiometry equals zero, and the best feed composition for the kinetics part of this reaction system is

$$\left(\frac{N_{H2}^0}{N_{CO}^0}\right)_{best} = \frac{\alpha}{\beta} = 2 \tag{31}$$

This is the same as the best feed composition for TDF and independent of the extent of the reaction. Therefore, methanol synthesis is a simple reaction system, and the best H_2:CO ratio in the feed will always be 2. The analysis agrees well with the observations from our computer simulation using Equation 30 and a well-mixed reactor model (see the LPMEOH^{TM} curve in Figure 2). It is also consistent with what is well understood in the methanol industry.

Syngas-to-Methanol Reaction System <u>with</u> Water Gas Shift Reaction

If the feed syngas contains a significant amount of CO_2 and/or water, the water gas shift reaction assumes importance, and the methanol synthesis process becomes a two-reaction system (Equations 1 and 3). The equations derived above no longer apply to this multi-reaction system. However, we will demonstrate that the two-term approach can still be used to provide the equations for calculating the best reactor feed and insightful information.

Let us start with the mass balance. Assuming the reactor feed does not contain methanol, the initial and final compositions of the reaction system become

	H_2	CO	CH_3OH	H_2O	CO_2	
Initial	$(1-x)N^o$	xN^o	0	N^o_{H2O}	N^o_{CO2}	(32)
Final	$(1-x)N^o-2\xi_1+\xi_2$	$xN^o-\xi_1-\xi_2$	ξ_1	$N^o_{H2O}-\xi_2$	$N^o_{CO2}+\xi_2$	(33)

where ξ_1 and ξ_2 are the extent of reaction for methanol synthesis and water gas shift, respectively.

Before the two-term approach for a multi-reaction system can be used, the optimization must be targeted at one of the reactions. Since the product of interest in this case is methanol, the methanol synthesis reaction is the target reaction. Therefore, the problem again becomes to maximize the rate shown by Equation 30.

First, let us analyze the best feed composition for TDF. Applying Equation 13 to this case, one has

$$\left.\frac{\partial DF}{\partial x}\right|_{\xi_1} = -\left.\frac{\partial (appr.)}{\partial x}\right|_{\xi_1} = -\frac{\partial}{\partial x}\left(\frac{p_{CH3OH}}{K_m p_{H2}^2 p_{CO}}\right) = 0 \tag{34}$$

Solving Equation 34 one obtains

$$\left(\frac{p_{H2}}{p_{CO}}\right)_{best} = BR = 2 \tag{35}$$

Substituting Mass Balance Equation 33 into Equation 35 gives

$$\left(\frac{N^0_{H2}}{N^0_{CO}}\right)_{best} = 2\left(\frac{1-\frac{3}{2}\frac{\xi_2}{N^0}}{1+3\frac{\xi_2}{N^0}}\right) \tag{36}$$

Now let us look at the best feed for RFR. Applying Equation 12 to this case one has

$$\left.\frac{\partial RFR}{\partial x}\right|_{\xi_1} = \left.\frac{\partial (p_{H2}^{\alpha} p_{CO}^{\beta})}{\partial x}\right|_{\xi_1} = 0 \tag{37}$$

Solving Equation 37 one obtains

$$\left(\frac{p_{H2}}{p_{CO}}\right)_{best} = BR = \frac{\alpha}{\beta} = 2 \tag{38}$$

Substituting Mass Balance Equation 33 into Equation 38 gives

$$\left(\frac{N_{H2}^0}{N_{CO}^0}\right)_{best} = \frac{\alpha}{\beta}\left(\frac{1-\frac{3}{2}\frac{\xi_2}{N^0}}{1+3\frac{\xi_2}{N^0}}\right) = 2\left(\frac{1-\frac{3}{2}\frac{\xi_2}{N^0}}{1+3\frac{\xi_2}{N^0}}\right) \tag{39}$$

which is the same as Equation 36. This is expected, because α/β happens to be equal to a/b with the power law rate expression we use. Note that the BRs for the TDF (Equation 35) and RFR (Equation 38) in this two-reaction system are the same as those derived for a single reaction system (Equations 20 and 23). However, this is only a coincidence. In general, the extent of other reactions in a multi-reaction system would appear in BRs if the reactants in the target reaction are also involved in other reactions. This will be discussed in detail later.

The effect of the water gas shift reaction is apparent in the final results (Equations 36 and 39). A term similar to *FA* appeared, making the best feed a function of the extent of the water gas shift reaction, ξ_2. The physical meaning of this *FA* term is as follows. In the methanol-synthesis-only case, once H_2 and CO in the reactor feed are balanced or stoichiometric (H_2:CO =2), the ratio of the two reactants will not change as the reaction progresses, and the TDF will be maximal at any extent of the reaction. Since α/β happens to be equal to a/b in this case, the same explanation applies to RFR. However, in the current two-reaction system, the two reactants, H_2 and CO, are not only consumed by the methanol synthesis reaction, but also re-proportionated by the water gas shift reaction. Therefore, to satisfy the best ratio for the TDF (Equation 35) and RFR (Equation 38), one must adjust the reactor feed away from 2, depending on the extent of the water gas shift reaction (ξ_2). Equations 36 and 39 provide the formulations for this adjustment.

This discussion can be mathematically illustrated by rearranging Equation 33 or 36, which leads to

$$\frac{N_{H2}^0 + \xi_2}{N_{CO}^0 - \xi_2} = 2 \qquad (40)$$

Equation 40 indicates that every ξ_2 mole of water gas shift reaction adds ξ_2 moles of H_2 to the system and consumes ξ_2 moles of CO. Therefore, if ξ_2 is known, one can adjust the amount of H_2 and CO in the reactor feed accordingly to make the H_2:CO ratio in the reactor 2, which is the best ratio for methanol synthesis (cf. Equation 35 and Equation 38).

A module, as shown below, has been used in the methanol industry to describe the composition of the fresh syngas feed to the methanol synthesis reactor.

$$M = \frac{N_{H2}^0 - N_{CO2}^0}{N_{CO}^0 + N_{CO2}^0}$$

It is believed that an M value of 2 gives the best syngas composition. Note that the left-hand side of Equation 40 has the same form as the module, except that $-\xi_2$ is in place of N^o_{CO2}. To reconcile this difference, one must assume that all CO_2 in the feed gas would be shifted to CO under methanol synthesis conditions. As shown below, this assumption is not true. If the industrial module was formulated on this assumption, this module, at best, is only an approximation and an approximation applying only to H_2-rich feed gas.

We have observed in the lab that water gas shift is much more rapid than methanol synthesis. The reaction is practically at equilibrium under most conditions in that a further approach to equilibrium would have negligible effects on H_2 and CO concentrations. Therefore, for a H_2-rich feed gas containing CO_2 but no water, as in most industrial cases, ξ_2 can be calculated from Equation 35 or 36 and the equilibrium equation for the water gas shift reaction. This changes Equation 40 into

$$\frac{N_{H2}^0 - \lambda_1 N_{CO2}^0}{N_{CO}^0 + \lambda_1 N_{CO2}^0} = 2 \qquad \text{for } H_2\text{-rich syngas with } N^o_{H2O} = 0 \qquad (41)$$

where $\lambda_1 = 2/(2+K_w)$, with K_w being the equilibrium constant of the water gas shift reaction. Note that $K_w >> 2$ at methanol synthesis temperatures (e.g., $K_w = 83$ at 250°C). This means $\lambda_1 << 1$ and Equation 41 cannot be reduced to the conventional module. In other words, the feed module used by the methanol industry is only an approximation.

If the feed gas is CO-rich, containing water but no CO_2, one can obtain

$$\frac{N^0_{H2} + \lambda_2 N^0_{H2O}}{N^0_{CO} - \lambda_2 N^0_{H2O}} = 2 \qquad \text{for CO-rich syngas with } N^o_{CO2} = 0 \qquad (42)$$

where $\lambda_2 = K_w /(2+K_w) \approx 1$. This module has not been seen in the methanol synthesis literature because the current methanol process uses H_2-rich syngas. However, the more recently developed liquid phase methanol technology (LPMEOH^{TM}) can use CO-rich gas directly, and there will be occasions when water injection is needed as an additional hydrogen source. In this case, the module shown in Equation 42 defines the best feed composition.

3.2.4. The Best Feed Composition for the Syngas-to-DME Reaction System

The single-step syngas-to-DME process is carried out over a catalyst system that possesses methanol synthesis, water gas shift, and methanol dehydration capability. The process contains three simultaneous reactions as shown by Equations 1, 2, and 3. The additional methanol dehydration reaction provides a cross-link between the methanol synthesis and water gas shift reactions by consuming the product of methanol synthesis, methanol, and feeding the water gas shift reaction with one of its own products, water. This makes the system much more complex than the two-reaction system discussed above.

We have tried to understand the best H_2:CO ratio for this reaction system by simulations using the kinetic models for the three reactions, as discussed in Section 3.2. The products of interest in this case are DME and methanol. Therefore, the target reaction for optimization is the methanol synthesis reaction, and the target productivity is so-called methanol equivalent productivity (MEP). MEP is defined as the space time yield of methanol plus 2 times the space time yield of DME. As shown in Figure 8, for a feed containing only H_2 and CO, the best H_2:CO ratio varies with the space velocity, shifting from around 2 at high space velocity to around 1 at low space velocity. While the simulation provides the specific answers we need for the given conditions, it does not provide a general answer for a wide range of conditions, nor does it provide any mechanistic understanding.

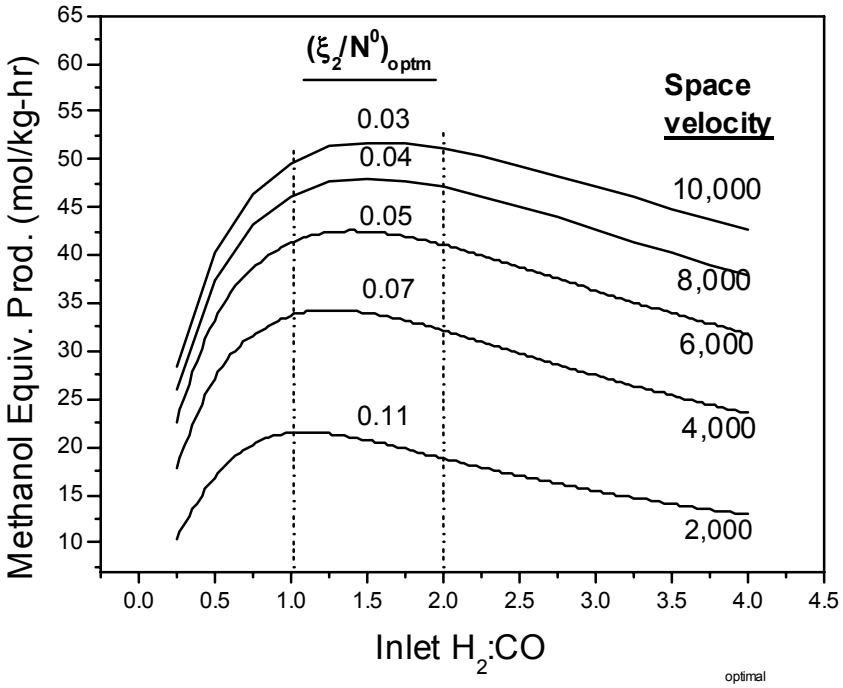

Figure 8: The methanol equivalent productivity as a function of the H_2:CO ratio in the reactor feed at different space velocities.

We will demonstrate in this section that the two-term approach can be applied to reaction systems as complex as the single-step syngas-to-DME reaction system. The equations for calculating the best feed composition for RFR and TDF can be obtained from the analysis. It provides additional insights into experimental and simulated observations such as those shown in Figure 8.

Let us start with the mass balance. For simplicity, we will use a feed that contains only H_2 and CO. The reactor feed and effluent compositions are

	H_2	CO	CH_3OH	DME	H_2O	CO_2	Total	
Feed	$(1-x)N^o$	xN^o	0	0	0	0	N^o	(43)
Effluent	$(1-x)N^o-4\xi_1+\xi_2$	$xN^o-2\xi_1-\xi_2$	$2(\xi_1-\xi_3)$	ξ_3	$\xi_3-\xi_2$	ξ_2	$N^o-4\xi_1$	(44)

ξ_1, ξ_2 and ξ_3 in Mass Balance Equation 44 are the extent of reaction for methanol synthesis, water gas shift and methanol dehydration, respectively. Note that ξ_1 is defined based on the stoichiometry shown in the following reaction equation:

$$4H_2 + 2CO \Leftrightarrow 2CH_3OH \qquad (45)$$

As mentioned above, both DME and methanol are desired products, and the target reaction in this three-reaction system is the methanol synthesis reaction. The problem then becomes similar to that in the syngas-to-methanol cases discussed above. That is, one must solve Equations 12 and 13 for the power law rate expression shown in Equation 30.

The Best Feed for the Kinetics

Let us first examine the best H_2:CO ratio in the reactor feed for the RFR. Solving Equation 12 at a fixed ξ_1 along with the RFR part in Equation 30, one obtains BR

$$\left(\frac{p_{H2}}{p_{CO}}\right)_{best} = BR = \frac{\alpha}{\beta} = 2 \tag{46}$$

Combining Equation 46 with Equation 44yields the best H_2:CO ratio in the reactor feed for the RFR, namely

$$\left(\frac{N^0_{H2}}{N^0_{CO}}\right)_{best} = 2\left(\frac{1-\frac{3}{2}\frac{\xi_2}{N^0}}{1+3\frac{\xi_2}{N^0}}\right) \tag{47}$$

The results shown in Equations 46 and 47 are the same as those in the syngas-to-methanol-with-water-gas-shift case (Equations 38 and 39). For the same reason as that discussed in the previous methanol-synthesis-plus-water-gas-shift case, ξ_2 appears in the feed adjustment term (FA). Note that the extent of the methanol dehydration reaction, ξ_3, has no effect on deriving Equation 46 and does not appear in FA. This occurs because the reaction does not involve H_2 and CO, and RFR is only a function of H_2 and CO. Furthermore, the dehydration reaction does not change the molar amount of total species in the system. Without these two coincidences, Equations 46 and 47 would have been more complex.

Equation 47 shows that the best H_2:CO ratio in the reactor feed is 2 for $\xi_2 = 0$, and the ratio decreases with increasing ξ_2. In principle, the lower boundary of this ratio can be obtained if one knows the value of ξ_2 at equilibrium. However, it is difficult to do so analytically because it requires solving four non-linear equations simultaneously (three equilibrium equations plus Equation 47). However, one can plot Equation 47 as a function of ξ_2 to visualize how the best feed ratio for RFR changes with ξ_2. As shown in Figure 9, the best ratio in the feed for RFR is a strong function of ξ_2, approaching a value of 1 quickly as ξ_2 increases. Figure 9 shows the ξ_2/N^o value as a function of space velocity under some typical syngas-to-DME reaction conditions, where Subscript *optimal* means that the ξ_2/N^o value corresponds to the best feed ratio for the given space velocity.

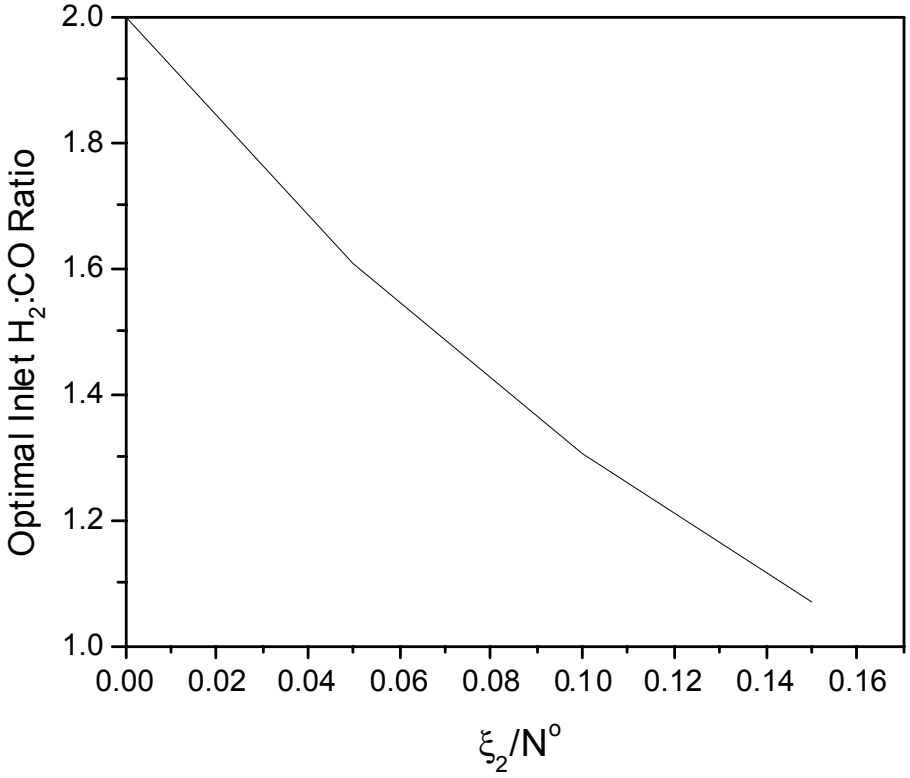

Figure 9: The best H_2:CO ratio for the kinetics of the syngas-to-DME system as a function of the extent of the water gas shift reaction.

The Best Feed for the Thermodynamics

Solving Equation 13 at a fixed ξ_1 along with the DF part of Equation 30, one obtains the BR for the TDF as

$$\left(\frac{p_{H2}}{p_{CO}}\right)_{best} = BR = 2\left(1 - \frac{\partial\xi_3 / \partial x}{N^0 - \partial\xi_2 / \partial x}\frac{p_{H2}}{p_{CH3OH}}\right) \tag{48}$$

Note that the BR is no longer simply equal to 2, as in the previous two cases. It is now a function of the extent of the other two reactions, ξ_2 and ξ_3. This occurs because methanol, which appears in *appr*., no longer drops out during optimization. Instead, it is a function of the methanol dehydration reaction, which in turn is a function of the water gas shift reaction. Although Equation 48 illustrates the coupling among three reactions, it does not provide the numerical answer for the BR. However, it does show that the BR for the TDF is less than 2, since the term in parentheses must be greater than zero. This indicates that the presence of the other two reactions shifts the BR for the TDF toward a more CO-rich regime.

Unfortunately, an analytical solution more explicit than Equation 48 cannot be obtained, so it is not possible to determine how the BR for the TDF in this system is affected by the other two reactions or to derive an equation for calculating the best feed composition for the TDF. Even solving Equation 13 numerically for this reaction system is a formidable task. As shown in Equation 48, this would involve calculating the extent of the other two reactions and how they vary with the feed composition. This requires a knowledge of the kinetics of the other two reactions. However, as discussed in Subsection 3.2.1, maximizing the TDF (Equation 13) is equivalent to maximizing the equilibrium extent of the reaction (Equation 14). This means that one can calculate the *equilibrium* syngas conversion of this reaction system as a function of the H_2:CO ratio in the reactor feed. The feed composition that gives the maximum equilibrium syngas conversion will also be the composition that gives the best TDF. In this equivalent approach, one needs only to solve the equilibrium equations for the three reactions simultaneously, without knowing the kinetics of the other two reactions. This calculation has been conducted numerically (Ref. 10 and the equilibrium curve in Figure 3). It shows that the maximum equilibrium syngas conversion is achieved at a H_2:CO of 1. That is, the best feed composition for the TDF of the methanol synthesis reaction in this system is

$$\left(\frac{N_{H2}^0}{N_{CO}^0}\right)_{best} = 1 \tag{49}$$

The Best Feed for the Reaction

It would be even more difficult to derive an equation for the best feed composition for the overall rate of the reaction. However, Equation 49 shows that the best H_2:CO ratio in reactor feed for the TDF is 1. Figure 9 shows that the best feed ratio for the RFR is 2 at very low conversion, but as the reactions proceed, it quickly approaches 1. Therefore, as we have observed in the simulation results shown in Figure 8, the expected best ratio for the reaction is between 2 and 1, but closer to 1 for a reasonable conversion. We now understand why the H_2:CO ratio in the feed for the maximum productivity shifts from 2 at high space velocity toward 1 with decreasing space velocity.

3.2.5. Discussion

At the heart of the two-term approach is a concept introduced in the above discussion: the best ratio of the reactants in the reactor or under reaction conditions (*BR*). It can be generally stated that, for a given reaction, there is a composition of the reactants (or a ratio of reactants for two-reactant systems) under the reaction conditions that gives the maximum rate of the reaction. Once this composition, or BR, is known, one can always satisfy it by adjusting the feed composition through simple mass balance. However, the best composition under the reaction conditions, or BR, for the overall rate of the reaction is often a function of the extent of reaction, and is difficult to determine. This is illustrated by the results shown in Equation 28 for the general single reaction system. The BR for the overall rate of the reaction shifts between the BR for the RFR and the BR for the TDF, depending on the approach to equilibrium (the extent of reaction).

The problem becomes better defined and easier to solve when the reaction rate is separated into its two essential components, the TDF and the RFR. For the single reaction system, the BR for the TDF is determined by the reaction stoichiometry or the thermodynamics, independent of the extent of the reaction (cf., Equation 20). The same holds true for multi-reaction systems if the products of the target reaction are not involved in the other reaction. Otherwise, the BR for the TDF, in principle, will be a function of the extent of the other reactions in the system. Even in this case, the problem is still defined by the thermodynamics and can be solved when the kinetics of all reactions are not known. This is clearly illustrated in the analysis of the syngas-to-DME reaction system.

For the single reaction system, the BR for the RFR is the property of the reaction only, independent of the extent of the reaction (cf., Equation 23). It can be derived analytically or numerically if the mathematical form of RFR is known, or it can be measured experimentally. If the reactants in the target reaction of multi-reaction systems are not involved in the other reactions in the system, for the target reaction, the BR for the RFR will be independent of the extent of all the other reactions in the system. Otherwise, it will be a function of the extent of the other reactions. The problem will then become more complex, except in some special cases.

One such special case is the methanol synthesis reaction in the methanol-synthesis-with-water-gas-shift reaction system and the syngas-to-DME reaction system. Although both reactants for methanol synthesis, H_2 and CO, are involved in the water gas shift reaction, the BR for the RFR in both cases is independent of the extent of the water gas shift reaction (cf., Equations 38 and 46). This, however, is a result of three coincidences. First, the water-gas-shift reaction does not change the total molar amount of the species in the reaction system. Second, the partial pressure of methanol, which is the product of the targeted reaction for optimization, is not affected by the water-gas-shift reaction. Third, although both H_2 and CO depend on the extent of the water-gas-shift reaction, their sum does not. Therefore, for a given extent of the methanol synthesis reaction, (P_{H2} + P_{CO}) is a constant. How this total amount is partitioned between P_{H2} and P_{CO} to give a maximal $p_{H2}^{\alpha} p_{CO}^{\beta}$ for the RFR and a maximal $p_{H2}^{a} p_{CO}^{b}$ for the TDF is not a function of the extent of the water gas shift reaction.

The linkage of the BRs for the TDF and the RFR to their best feed composition is simple mass balance. For single reaction systems, the BR for the TDF agrees with the ratio defined by the reaction stoichiometry. Therefore, the stoichiometric or balanced feed gives the maximum TDF. This feed gas composition will not change with the extent of reaction, and the BR for the TDF will always be satisfied. In contrast, the BR for the RFR is often different from the ratio defined by the reaction stoichiometry. That is, *Deviation* may not be zero. Therefore, the ratio of the two reactants in the reactor feed needs to be adjusted (*FA*) so that the BR can be obtained at the targeted extent of reaction. In the process of converting the BR to the best reactor feed composition, generally the extent of other reactions will be introduced into the final equations. However, once the BR is known, the equations for the best feed composition can be readily obtained.

General equations for the BR and best feed composition have been derived from the two-term approach for single-reaction systems. The problem is more complex for multi-reaction systems;

hence, the results become case-specific. We have applied the two-term approach to the methanol-synthesis-with-water-gas-shift reaction system (2 reactions) and the syngas-to-DME reaction system (3 reactions). Useful results have been obtained, although a numerical solution has to be used in the latter case. In all cases, dealing with the two components individually makes the mechanistic understanding possible and mathematical derivations simpler. Determining the usefulness of this approach to multi-reaction systems in general requires examination of more reaction systems. Mention should be made that the results for the TDF part, in all of the above cases, should be close to reality, since the reaction stoichiometries are well defined, and the equilibrium constants are reliable. The results for the RFR part, in terms of reflecting the reality, are only as good as the power law rate expression we have used in the analysis.

The approach developed in this work essentially is the analysis of the best starting composition for a reaction for a given extent of reaction. For a well-mixed reactor under steady-state operation conditions, this is equivalent to analysis of the best reactor feed composition for the reactor productivity. For this type of reactor, the extent of reaction is a fixed number. For a plug flow reactor or a batch operation, the extent of reaction changes with the position in the reactor or the time of operation. Unless the BRs for both the TDF and the RFR agree with the reaction stoichiometry (for example, a methanol synthesis-only case), the analysis cannot be applied directly.

4. The Schemes for the Syngas-to-DME Process Based on the Best Reactor Feed

The principal incentive for developing a single-step syngas-to-DME process is to produce DME at a cost lower than that of the commercial two-step production process of syngas-to-methanol followed by methanol dehydration carried out in sequential reactors. The cost penalties of the two-step process are (1) limited productivity in the syngas-to-methanol reactor due to equilibrium constraints and (2) the need for a second dehydration reactor and associated separation units. The single-step syngas-to-DME reaction system allows greater productivity in a single reactor system because of the synergy among the three reactions. However, downstream separation in the single-step process is more complex and costly. This trade-off makes it necessary to optimize the productivity of the reactor in order to produce DME at a lower cost. In other words, the one-step process will be able to produce DME at a cost lower than the two-step process only if the methanol equivalent productivity of the reactor in the one-step process is sufficiently greater than the methanol productivity in the two-step process,

It was demonstrated in the last section that the productivity of the syngas-to-DME reactor is a strong function of the feed gas composition (H_2:CO ratio). For a syngas feed containing only H_2 and CO, the maximum methanol equivalent productivity is obtained at a H_2:CO ratio of around 1. Note that this observation is obtained for once-through operation. It poses an interesting challenge of how to incorporate this observation into process development that involves recycle.

The first part of the current section demonstrates that, for the process involving various recycle schemes, a possible best choice for the overall reaction is, again

$$3H_2 + 3CO \rightarrow CH_3OCH_3 + CO_2 \quad (4)$$

This can be achieved by recycling methanol and water along with the unconverted syngas. The method is a design choice, since the overall reaction scheme in a process with recycle can be done in many different ways. The detailed reasoning for choosing this overall reaction will be given below. In brief, given the right feed gas composition at a H_2:CO ratio of 1:1, this configuration results in optimal DME productivity and materials utilization, and therefore could be a good basis for future commercial processes. Furthermore, this example demonstrates the importance of feed gas composition in developing one-step syngas-to-DME processes.

The second part of this section deals with the issues associated with the overall reaction shown in Equation 4. This design choice sacrifices one third of the carbon in the syngas to CO_2. This means low carbon utilization. Generation of CO_2 in the process may also be an environmental concern, since CO_2 is a greenhouse gas. The second issue associated with the reaction scheme is the mismatch between the best syngas gas composition for this configuration (H_2:CO ratio of 1:1) and the composition of the syngas that can be generated by commercially available conversion units. The H_2:CO ratio from most syngas generation units is not 1:1, except for the case of the CO_2-methane reformer. For coal-derived, CO-rich syngas, this problem can be solved readily by injecting water into the reactor to provide the extra hydrogen through the water gas shift reaction. However, lowering the hydrogen content in natural gas-derived, H_2-rich syngas is not straightforward. In the second part of this section, we propose the process concepts and schemes that result from integration of the syngas-to-DME reaction with syngas generation units. The overall reaction is shown in Equation 4. This integration simultaneously solves the above-mentioned two problems. We further demonstrate through simulations that these process schemes encompass commercially relevant conditions. With these process schemes to eliminate CO_2 emissions and derive 1:1 syngas and with the syngas-to-DME reactor running at the optimal productivity, we believe that one can develop commercially cost-effective, one-step, syngas-to-DME processes that produce DME.

4.1. Simulation Details

The details about the kinetic models and the reaction conditions for the syngas-to-DME reactor are the same as those given in Section 2. Commercially relevant conditions were used for simulations of syngas generation units. The CO_2-methane reformer and the steam methane reformer were simulated by thermodynamic equilibrium model. The methane partial oxidation reactor was modeled with a kinetic model that is based on our knowledge of the commercial performance of the reactor. The detailed information for each simulation is given when a specific example is discussed. The separation units were simply specified to provide the desired separation; all separations can be achieved using commercially available technologies. The ASPEN PLUS process-simulating package was employed in all simulations.

4.2. Selection of a Recycle Scheme and Overall Reaction

Choosing a process configuration with recycle for our study is a complex issue. Recycle introduces additional variables such as recycle-to-feed ratio and the choices of species to be recycled. Different selections give different kinetic performance and overall reactions. Our criteria in selecting the recycle scheme are (1) the best productivity in the syngas-to-DME

reactor and (2) a simple, well-defined yet commercially relevant overall reaction for our kinetic study and conceptual development of process schemes.

First, reactor feed ratios of H_2:CO less than 1.5 were chosen, since this is the region where the chemical synergy becomes significant and great productivity improvements can be obtained. The choice of species for recycle is complex, since the reactor effluent contains CO_2, water, and methanol as well as unconverted syngas. Due to the imbalance in the carbon-to-oxygen ratio between the feed (1:1 in CO) and the product (2:1 in DME), the extra oxygen must be rejected either as CO_2, H_2O, or both. In this study we chose to reject CO_2. In the regime of interest (H_2:CO <1.5), CO_2 is formed in large excess to water. Recycling CO_2 to the reactor to convert the excess oxygen to water would have accumulated a large amount of CO_2 in the recycle loop due to the shortage of H_2. A high concentration of CO_2 would hurt the chemical synergy, and therefore, DME productivity, by (1) diluting the feed and (2) building up water in the reactor, as shown in Section 3.1.

Our chosen scheme includes water and methanol in the recycle loop, along with the unconverted syngas. As shown below, recycling water and methanol has little impact on the kinetics of the reaction system for the regime of interest (H_2:CO <1.5). Thus the choice simplifies the overall reaction into a well-defined form (Equation 4) without narrowing the validity of the study. Furthermore, methanol and water recycle may also be a practical arrangement. It avoids dealing with methanol as an undesired by-product or using a second reactor to convert methanol to DME and avoids separation of water from methanol.

The process configuration based on these selections gives the overall reaction shown in Equation 4. It has the potential to provide optimal productivity and may form a good base for developing commercial one-step syngas-to-DME process packages. Furthermore, it is simple, and therefore useful, for our kinetic study, especially for conceptual developments of process schemes. Based on our understanding of the reaction system as discussed in Section 3, this is a configuration that has good commercial potential. Our selection of this process scheme does not imply that it is the only configuration that will meet our stated objectives.

4.3. Dependence of DME Productivity and Material Utilization on the Feed Gas Composition in the Recycle Case

This sub-section demonstrates how DME productivity depends on the feed gas composition in the recycle case. The results are obtained through simulations. The process diagram used in the simulation is shown in Figure 10.

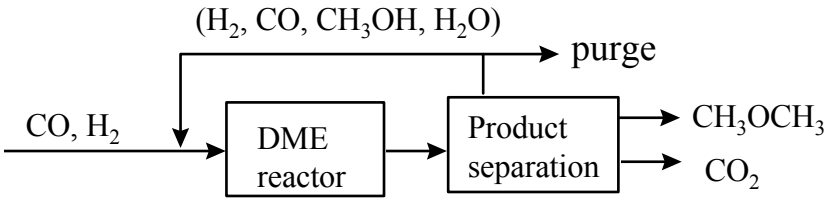

Figure 10: DME production from syngas with syngas, methanol and water recycle.

The purge stream is used to avoid building up too large a recycle stream of inerts. The fresh feed contains only H_2 and CO. The reaction conditions are 250°C, 5.2 MPa, and 2000 sl/kg-hr total feed (fresh feed plus recycle). The recycle-to-purge ratio is set at 4:1. The H_2/CO ratio in the feed was varied.

The results from this simulation are shown in Figure 11. A very strong dependence of the DME productivity on the H_2:CO ratio in the FRESH feed gas is observed. The maximum productivity (10.9 mol/kg-hr) occurs at a H_2:CO ratio of 1.0. The productivity drops by about 65% and 44% when the ratio changes to 0.5 and 1.5, respectively. This demonstrates the importance of feed gas composition in process design.

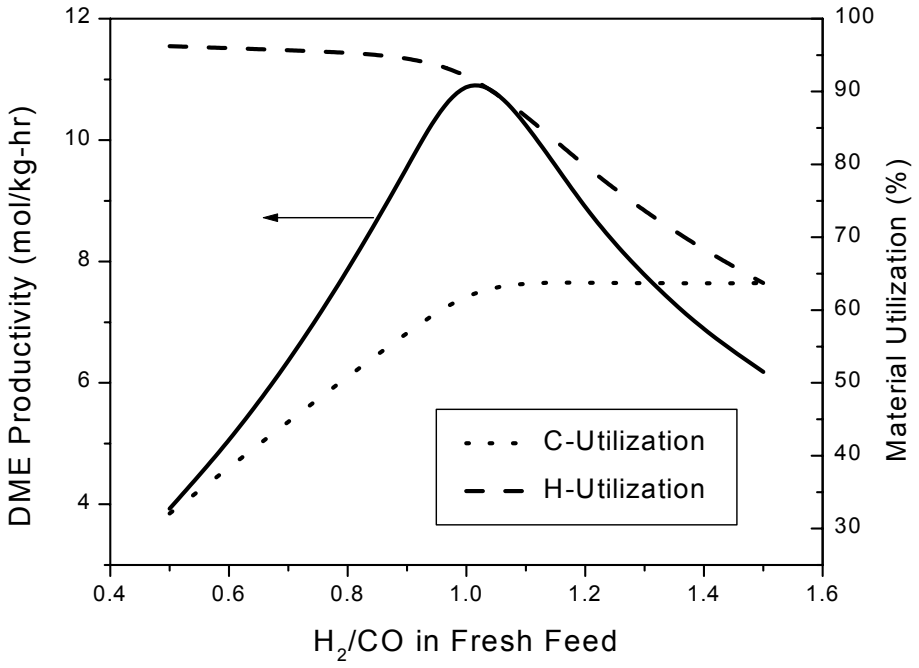

Figure 11: The effect of H_2:CO ratio on DME productivity and materials utilization.

Figure 11 also shows the carbon and hydrogen utilization, or the molar fraction of the carbon or hydrogen in the fresh syngas feed incorporated into DME, as a function of the H_2:CO ratio in the fresh reactor feed. The carbon and hydrogen utilization by Reaction 4 with no purge would be 67% and 100%, respectively. The reduction of carbon utilization in the CO-rich range (H_2:CO <1) is due to the unbalanced feed. Insufficient H_2 in the feed causes CO to accumulate in the recycle loop, and from there, it is lost to the purge. Above 1:1, the carbon utilization approaches the expected value of 67%. However, hydrogen starts to accumulate in the recycle loop and is lost through the purge stream. Thus, hydrogen utilization decreases as H_2:CO ratio increases. Clearly, optimal overall materials utilization is achieved at a 1:1 H_2:CO ratio. This behavior is expected, as 1:1 is the stoichiometric feed for Reaction 4.

A more important feature revealed by the above simulation is the coincidence of the optimal H_2:CO ratio for the DME productivity with the stoichiometry of the overall reaction. In other words, both the best kinetics and material utilization occur at the same conditions. This doubles the incentive to run the syngas-to-DME reaction with a feed ratio of 1:1 H_2 to CO.

The earlier statement that methanol and water recycle have little effect on the reactor performance is verified by the results shown in Table 2. Table 2 lists the concentration of methanol and water in the reactor effluent at different H_2:CO ratios in the feed gas. Two sets of data are presented: one with, the other without methanol and water recycle. The concentration of both species varied only slightly from one case to the other, indicating that recycling methanol and water is a good simplification with little impact on the reaction system under study.

Table 2: The concentration of methanol and water in the reactor effluent at different H_2:CO ratios in the feed gas.

	with methanol and water recycle		without methanol and water recycle	
H_2:CO	CH_3OH mol.%	H_2O mol.%	CH_3OH mol.%	H_2O mol.%
0.5	0.045	0.003	0.044	0.003
1.0	1.33	0.34	1.09	0.26
1.5	4.46	2.90	4.14	2.26

4.4. Integration between the Syngas-to-DME Reactor and Syngas Generation Units

As discussed above, a design based on Reaction 4 generates CO_2, which is an environmental concern and lowers the economic return. Furthermore, the composition of most commercially available syngas (except that produced by a CO_2 methane reformer) is not the optimal composition (1:1 H_2:CO, as shown in Figure 11) for the syngas-to-DME reactor. Solutions to these two problems may allow Reaction 4 and the corresponding process configuration to serve as an attractive basis for commercial development. For coal-derived syngas, the mismatch in syngas composition can be fixed easily by introducing water into the reactor to provide the extra hydrogen. For natural gas-derived syngas, lowering the high H_2:CO ratio (normally ≥2, except the CO_2 reformer) to 1:1 is not straightforward. The solution appears when one considers the DME unit and syngas generation units together. Carbon dioxide, an undesired by-product from the DME reactor, can be recycled to a natural gas-based syngas generation unit (e.g., methane reformers and the methane partial oxidation reactor). Since all of these units possess water gas shift activity and an H_2-rich environment, CO_2 can be converted to CO, thus eliminating CO_2 emissions and lowering the H_2:CO ratio in the syngas. The benefits, working mechanism, and technical feasibility of the integration are shown below.

Numerous integration schemes can be constructed. Figure 12 shows a generic flow sheet consisting of three parts. The first part converts methane (natural gas) into syngas, with conversion being performed in a CO_2 methane reformer, a steam methane reformer, a methane partial oxidation reactor, or any combinations of these technologies. Accordingly, the feed to the unit (Stream 1) is methane plus CO_2, H_2O, or O_2, or some combination of the species. The second part is a coal gasifier and is used only when additional carbon is needed; the CO-rich

syngas (Stream 4) from this unit lowers the H_2:CO ratio in the overall feed to the DME reactor directly by combining with the normally H_2-rich syngas stream from the methane reformer and indirectly by forming more CO_2 in the DME reactor. The third part reacts syngas to DME, in exactly the same way shown in Figure 10. The separation unit converts the DME reactor effluent (Stream 6) into three streams containing unconverted syngas plus methanol and water (Stream 7), CO_2 (Stream 9), and product DME. The CO_2 stream is recycled to the methane converter and thus is no longer a by-product.

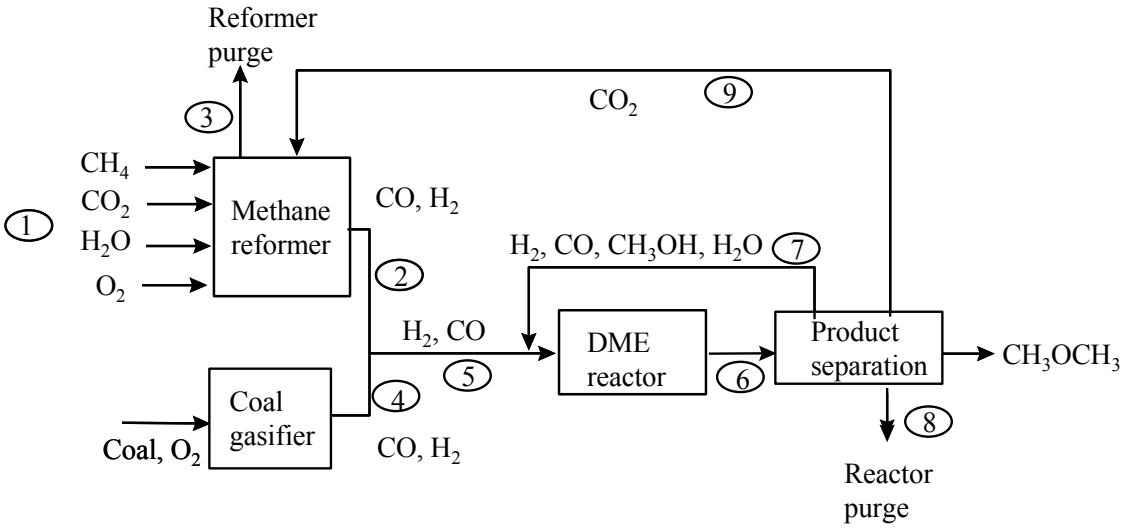

Figure 12: Integration of syngas-to-DME with syngas generation.

Specific integrations can be devised to fit process requirements and specific customer needs. The following four examples show the integration for specific situations. A conceptual demonstration based on overall mass balance was performed first to show the working mechanism of an integration, assuming that the reactions go to completion in each reactor. The demonstrations were followed by simulations using realistic reactors, kinetics, and thermodynamics to prove the technical feasibility. A small amount of N_2 was included in the fresh feed to the reformer to model the accumulation of inerts in the loop. The coal gasifier was simulated as a syngas source with a specified composition. The operating conditions for the syngas-to-DME loop were kept the same in all examples and were identical to those described in the base case (Section 4.3). It should be pointed out that none of the examples was optimized with respect to operating temperature and pressure, ratio of recycle-to-feed and recycle-to-purge, space velocity, inert content of the gas streams, and so forth. The objective was purely to demonstrate the advantages and technical feasibility of the integration.

4.4.1. Syngas-to-DME + CO_2 Methane Reformer

In theory, a CO_2 methane reformer produces a balanced syngas (H_2:CO =1) according to the equation below:

$$CH_4 + CO_2 \rightarrow 2CO + 2H_2 \qquad (38)$$

This, however, requires a CO_2 source to match every CH_4 with a CO_2, a requirement that adds to the cost of this reforming technology. Integration by recycling CO_2 from the DME unit to the CO_2 reformer (Figure 13) reduces this requirement to one fresh CO_2 for every three of CH_4. DME is the only product from this integration. The overall reaction is

$$3CH_4 + CO_2 \rightarrow 2CH_3OCH_3 \qquad (39)$$

A similar scheme has been proposed by Shikada et al. [18].

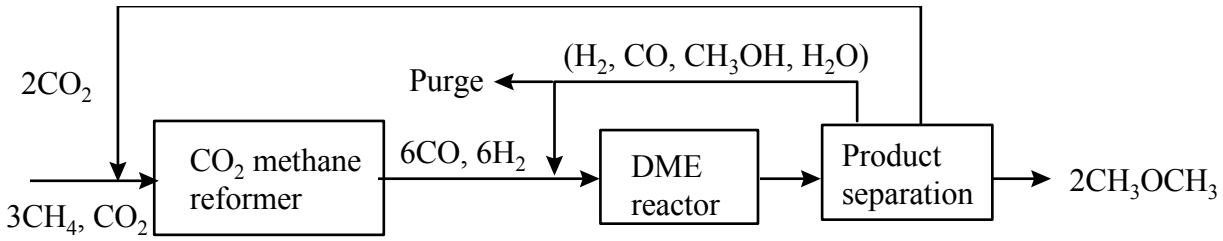

Figure 13: Integration of syngas-to-DME with CO_2 methane reformer.

In deriving Equation (39), we assumed full conversion of methane and CO_2 in the reformer and syngas in the DME reactor. The following simulation shows that these requirements can be approached in a reformer operated under commercially relevant conditions.

The reformer is modeled by thermodynamic equilibrium, with the pressure set at 200 psig and the temperature ranging from 782 to 927°C. The temperature range and pressure were selected to keep the reactor heat transfer tubes operating within safe limits. The CO_2:CH_4 ratio in the fresh feed (0.4) is held slightly higher than that shown in Figure 13 (0.33) in order to enhance CH_4 conversion and mitigate carbon deposition in the reformer. An internal recycle loop in the reformer section of the integration sends unconverted CO_2 and product H_2O back to the reformer. Because the fresh feed is slightly CO_2-rich, this recycle accumulates CO_2 and H_2O in the loop, enhancing CH_4 conversion and mitigating carbon deposition. The ratio of this internal recycle to the fresh feed is set at 1.5:1. No attempt is made to recycle unconverted CH_4. The CH_4 slip from the reformer is simply sent to the DME reactor along with the syngas, and eventually leaves the system through the DME reactor purge. The conditions for the DME reactor are the same as those used in the stand-alone case as described in Section 4.3. A CO_2 separator with 100% selectivity is used to separate CO_2 from the DME reactor effluent and to recycle it back to the reformer. The simulated composition and mole flow in each stream in this process scheme are summarized in Table 3.

Table 3: Simulated results (in moles; cf., Figure 12 for stream ID)

Stream Description	Stream ID	H_2	CO	CO_2	N_2	MeOH	DME	H_2O	CH_4
Fresh reformer feed	1	0	0	40	1	0	0	0	100
Reformer effluent	2	186	190	0	1	0	0	0	5.9
Recycle to reformer	9	0	0	57	0	0	0	0	0
Reformer purge	3	0	0	1.2	0	0	0	1.8	0
Fresh DME reactor feed	5	186	190	0	1	0	0	0	5.9
DME reactor effluent	6	60	86	57	5	2.4	58	0.6	30
DME reactor recycle	7	48	68	0	4	1.9	0	0	24
DME reactor purge	8	12	17	0	1	0.5	0	0	6.0

The methane and CO_2 per pass conversion in the reformer are 94% and 52%, respectively, and the steam-to-CH_4 and CO_2-to-CH_4 ratios in the overall feed to the reformer are 1.2 and 1.8, respectively. The equilibrium is outside the carbon deposition zone at 732°C. These conditions are well suited for a dry reformer such as that in the SPARG process. The syngas feed generated by the reformer contains 48.4 mol.% H_2 and 49.6 mol.% CO, plus 1.5 mol.% slipped CH_4 and 0.3 mol.% of spiked N_2. This mixture is close to the 1:1 requirement for the DME reactor.

The recycle-to-purge ratio in the syngas-to-DME reactor is set at 4:1, as in the stand-alone case shown in Section 4.3. The resulting recycle-to-feed ratio is 0.3:1. The per-pass and total syngas conversion in the DME reactor are 70 and 92%, respectively, and the reactor operates at a productivity of 9.7 gmol DME/kg-hr. This is slightly less than that in the stand-alone case (10.9), mainly due to the dilution of the reactor feed by CH_4. Sixty-one percent of the CO in the fresh feed to the reactor is converted to DME, which is close to the theoretical value of 67% (see Equation 4). The overall "carbon utilization," the carbon in the methane and CO_2 in the fresh feed to the reformer that is eventually incorporated in DME, is 82.1%. The integration emits no CO_2. The major carbon loss is due to unconverted CH_4 in the reformer and CO in the DME reactor. The overall hydrogen utilization is 87%, with the rest lost to the purge stream of the DME reactor.

There is good agreement between the simulated results and the conceptual stoichiometry shown in Figure 13, except for several minor differences. These include a slightly higher CO_2:CH_4 ratio in the fresh feed to the reformer mentioned above and smaller amounts of recycled CO_2 and product DME due to less than 100% conversion in the DME reactor.

4.4.2. Syngas-to-DME + CO_2 Methane Reformer + Coal Gasifier

The highly productive DME process discussed in Section 4.4.1 produces DME from methane with minimal emissions. However, it requires a supplementary CO_2 source. This need for CO_2 can be satisfied as shown in Figure 14. In order to understand this process scheme, let us first look at the simple combination of a DME unit with a coal gasifier. Assuming that (1) syngas feed to the DME reactor is CO-rich and consists solely of H_2 and CO, 2) water is injected to the DME reactor to provide the extra hydrogen, 3) all syngas is converted in the DME reactor and 4) methanol and unconverted water are fully recycled along with unconverted syngas, the overall reaction becomes

$$6CO + 6RH_2 + 3(1-R)H_2O \rightarrow (1+R)CH_3OCH_3 + 2(2-R)CO_2 \qquad (40)$$

where R is the H_2:CO ratio in the coal-derived syngas and ranges from zero to one. This equation is similar to Reaction 4 in that it produces only DME and CO_2. Water injection provides additional hydrogen for more DME formation. However, it also produces an extra amount of CO_2 to eliminate the oxygen originally introduced to the reactor by water.

Since Reaction 40 produces CO_2 and the process shown in Figure 13 needs CO_2, these two can be combined beneficially as shown in Figure 14. The overall reaction for this integration is:

$$2(2-R)CH_4 + 2CO + 2RH_2 + (1-R)H_2O \rightarrow (3-R)CH_3OCH_3 \qquad (41)$$

This scheme forms a self-sufficient system with a feed mixture of methane, coal, O_2, and water, and DME as the only product; there are zero emissions. Since the process requires both a CO_2 reformer and a coal gasifier, the investment may be considerable. However, the process may be well suited for a site that has both natural gas and coal resources, such as in the case of utilization of methane from coal mines.

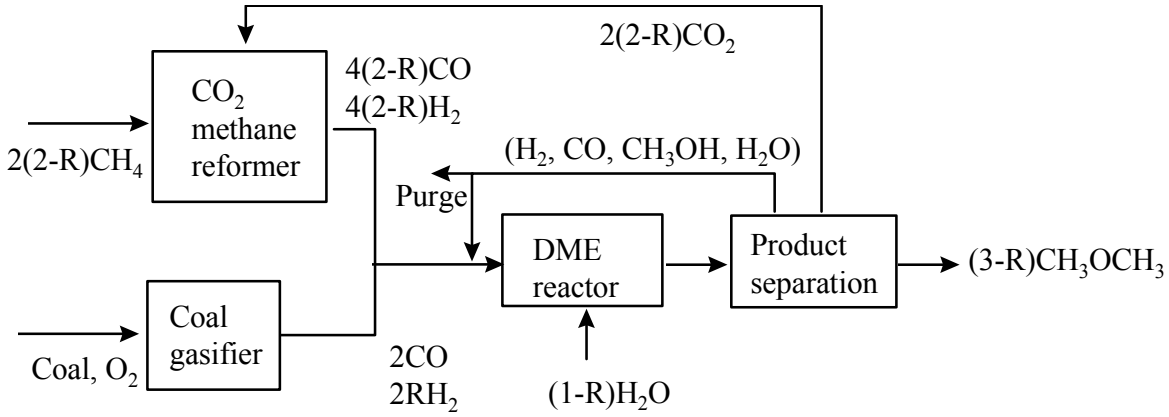

Figure 14: Integration of the syngas-to-DME unit with a CO_2 reformer and a coal gasifier.

Simulation results for this process scheme are summarized in Table 4. Two minor modifications were made in the simulation. First, the Shell-type coal gasifier is simulated. The Shell-type syngas contains some CO_2 and N_2 (3 and 1 mol.%, respectively) in addition to CO and H_2 (66 and 30 mol.%, respectively). Second, water is injected into the reformer, instead of into the syngas-to-DME reactor. This injection scheme enhances methane conversion and mitigates coke formation in the reformer. It also reduces dilution in the feed to the DME reactor. The reformer conditions are the same as provided in the last section, namely 782 to 927°C; 200 psig; 1:5:1 internal CO_2 and H_2O recycle; zero CH_4 recycle; and equilibrium control. The DME reactor again operates at the same conditions as those specified in the stand-alone case. The simulated composition and molar flow in each stream in this process scheme are summarized in Table 4.

Table 4: Simulated results (in moles; cf., Figure 12 for stream ID)

Stream Description	Stream ID	H_2	CO	CO_2	N_2	MeOH	DME	H_2O	CH_4
Fresh reformer feed	1	0	0	0	1	0	0	25	102
Reformer effluent	2	210	167	0	0	0	0	0	7.5
Recycle to reformer	9	0	0	75	0	0	0	0	0
Reformer purge	3	0	0	1.8	0	0	0	3.2	0
Coal-derived syngas	4	30	66	3	1	0	0	0	0
Fresh DME reactor feed	5	240	233	0	2	0	0	0	7.5
DME reactor effluent	6	96	76	75	10	4.6	73	1.3	38
DME reactor recycle	7	77	61	0	8	3.7	0	0	30
DME reactor purge	8	19.2	15.2	0	2	0.92	0	0	7.5

The methane and CO_2 per pass conversion in the reformer are 93% and 51%, respectively. The steam-to-CH_4 and CO_2-to-CH_4 ratios in the overall feed to the reformer are both 1.5. The reformer is outside the carbon deposition zone over the entire temperature range. Therefore, the operation is suited for a traditional steam methane reformer, as well as a dry reformer such as that in the SPARG process. Other important performance data are 93% overall syngas conversion and 9.8 gmol/kg-hr DME productivity; 86% overall carbon utilization; and zero CO_2 and H_2O rejection. The major material loss is due to unconverted CH_4 and syngas in the DME reactor purge.

The simulated results agree well with the conceptual stoichiometry shown in Equation 41. The overall feed to the reformer is balanced without a supplementary CO_2 source. The syngas feed generated by the reformer contains 49.7 mol.% H_2 and 48.3 mol.% CO (close to the 1:1 requirement for the DME reactor), plus minute amounts of CH_4 and N_2. Minor differences include 50% higher H_2O feed to enhance CH_4 conversion and mitigate coke formation in the reformer and 14% lower DME production due to incomplete conversion in the DME reactor.

4.4.3. Syngas-to-DME + Steam Methane Reformer + H_2 Product

The lowest H_2:CO ratio that can be achieved in a steam methane reformer (SMR) with full *internal* CO_2 recycle is 3:1 [19]. The next integrated process example recycles CO_2 from the DME unit to a SMR operating under this full internal recycle mode (Figure 15). The gas from the reformer with both internal and external CO_2 recycle will still be rich in H_2 (H_2:CO = 5:3). The non-stoichiometric H_2 can be separated to obtain a product H_2 stream and a balanced feed (H_2:CO of 1:1) for the DME reactor. The overall reaction for the integration is:

$$2CH_4 + H_2O \rightarrow CH_3OCH_3 + 2H_2 \qquad (42)$$

This integrated process scheme produces zero emissions. In principle, the extra hydrogen can be balanced by adding a coal gasifier to the process scheme. We chose the current configuration to show the flexibility and variations one can obtain through integration. Hydrogen may be a desired co-product for some applications. The hydrogen separation, a simple fractionation, may

be readily achieved using a H_2 membrane. This configuration is especially suited for a HYCO plant that sells H_2 and CO as products.

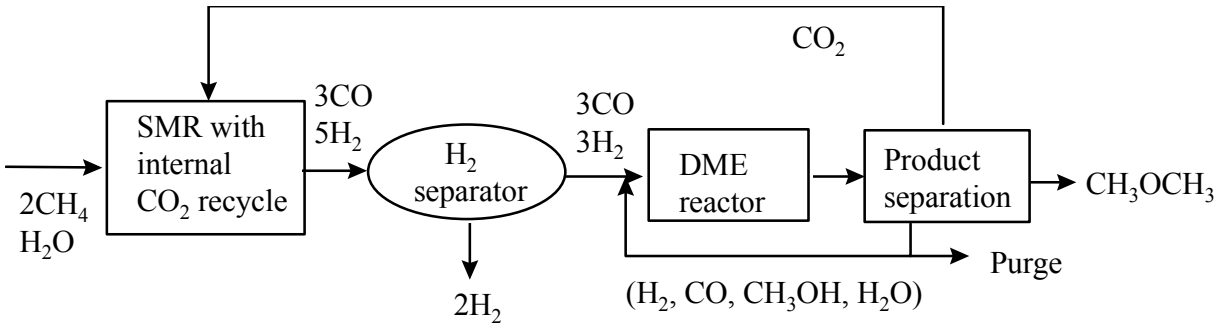

Figure 15: Integration of syngas-to-DME with a steam methane reformer.

Simulation conditions for this integration are the same as those used in the two examples above. The results from this simulation are summarized in Table 5. The H_2O-to-CH_4 ratio in the fresh feed to the reformer (0.6) is greater than that shown in Figure 5 (0.5). Again, the intent is to enhance methane conversion and mitigate coke formation. The resulting H_2:CO ratio (1.8), therefore, is higher than that shown in Figure 15 (1.7). The steam-to-CH_4 and CO_2-to-CH_4 ratios in the overall feed to the reformer are 2.4 and 1.1, respectively, and the equilibrium in the reformer is outside the carbon deposition zone over the entire temperature range. Among the other important performance data are 94.5% and 36% per pass conversion in the reformer for methane and CO_2, respectively; 93% syngas conversion; 9.7 gmol/kg-hr DME productivity in the DME reactor; 84% overall carbon utilization; and zero CO_2 emissions.

Table 5: Simulated results (in moles; cf., Figure 12 for stream ID)

Stream Description	Stream ID	H_2	CO	CO_2	N_2	MeOH	DME	H_2O	CH_4
Fresh reformer feed	1	0	0	0	1	0	0	60	100
Reformer effluent	2	139	135	0	1	0	0	0	5.5
Recycle to reformer	9	0	0	41	0	0	0	0	0
Reformer purge	3	105*	0	0.9	0	0	0	6.6	0
Fresh DME reactor feed	5	139	135	0	1	0	0	0	5.5
DME reactor effluent	6	54	46	41	5	2.5	42	0.7	28
DME reactor recycle	7	44	37	0	4	2.0	0	0	22
DME reactor purge	8	11	9.1	0	1	0.5	0	0	6

*: H_2 product.

4.4.4. Syngas-to-DME + Methane Partial Oxidation (POX)

Partial oxidation of methane typically produces syngas with a H_2:CO ratio close to 2:1. If CO_2 from the syngas-to-DME unit is fed to the POX reactor to enhance the reverse water gas shift reaction, the overall reaction for the integration, as shown in Figure 7, becomes

$$2CH_4 + O_2 \rightarrow CH_3OCH_3 + H_2O \qquad (43)$$

This integrated process produces a balanced syngas feed for the DME reactor and zero CO_2 emissions. However, one fourth of the hydrogen in methane ends up in water rejected from the POX.

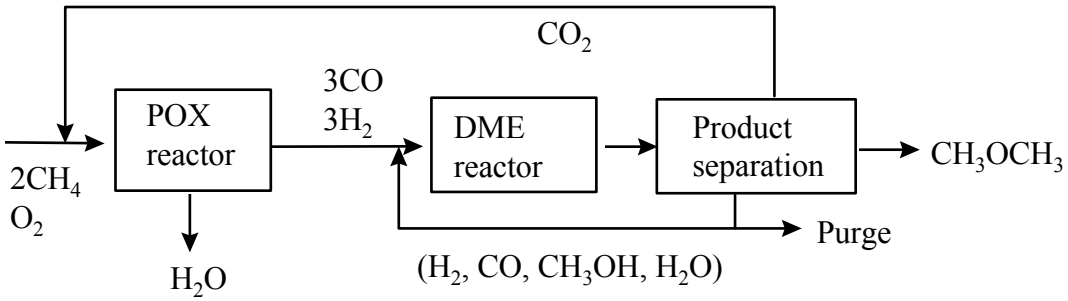

Figure 16: Integration of syngas-to-DME with a POX reformer.

The POX reformer is simulated as an adiabatic reactor and treated as a once-through operation. Typical commercial temperature (1316^{o}C) and pressure (350 psig) are used. The performance of the POX reactor is based on the conventional material balances that include 100% oxygen consumption and 0.4% CH_4 slip in the effluent (almost 100% CH_4 conversion). The extent of the water gas shift reaction is such that the ratio $([H_2][CO_2])/([H_2O][CO])$ in the effluent is equal to 0.5, as opposed to 0.33 of the equilibrium constant at the given temperature to account for the incomplete approach to equilibrium of the reaction. Again, the DME reactor is simulated under the same conditions used in the above examples. The results from the simulation are summarized in Table 6.

Table 6: Simulated results (in moles; see Figure 12 for stream ID)

Stream Description	Stream ID	H_2	CO	CO_2	N_2	MeOH	DME	H_2O	CH_4
Fresh reformer feed	1	0	0	0	1	0	0	50	101.5
Reformer effluent	2	156	144	20	1	0	0	0	1.5
Recycle to reformer	9	0	0	64	0	0	0	0	0
Reformer purge	3	0	0	0	0	0	0	44	0
Fresh DME reactor feed	5	156	144	20	1	0	0	0	1.5
DME reactor effluent	6	77	38	64	5	4.9	46	1.8	7.7
DME reactor recycle	7	61	31	0	4	3.9	0	0	6.2
DME reactor purge	8	15	7.7	0	1	1.0	0	0	1.5

The H_2:CO ratio in the POX effluent is 1.1, slightly greater than the expected value of 1, due to the incompleteness of the water gas shift reaction. The effluent contains CO_2 (5.5 mol.%). This CO_2 is fed directly, along with the syngas, to the DME reactor and recycled back to the POX reactor, along with the CO_2 formed in the DME reactor. Water (11.9 mol.% in the effluent), therefore, part of the hydrogen in the original CH_4, is removed downstream of the reformer before the syngas is fed to the DME reactor. The final fresh feed to the LPDME reactor consists of 48.2 mol.% H_2, 44.4 mol.% CO, 6.2 mol.% CO_2 and 0.3 mol.% N_2.

Due to the CO_2 in the fresh feed to the DME reactor, the DME productivity (9.5 DME mol/kg-hr) is lower than that in the stand-alone case (10.7). The overall syngas conversion in the DME reactor is 89% and the overall carbon utilization is 91%. The integration produces zero CO_2 emissions. The main materials loss is the unconverted syngas in the DME reactor purge.

4.5. Discussion

The performance of the syngas-to-DME reactor is a very sensitive function of the H_2:CO ratio in the fresh feed for syngas-to-DME processes that involve syngas recycle. The dependence of the DME productivity on the H_2:CO ratio in the fresh feed shown in Figure 11 is much stronger than expected from the once-through case (see Section 3). This arises since any deviation of the H_2:CO ratio in the fresh feed from the stoichiometry of the overall reaction (1:1) is amplified in the total feed (fresh plus recycled syngas) to the reactor because of the recycle. For example, for the fresh feed with H_2:CO ratios of 0.5, 1.0, and 1.5, the corresponding H_2:CO ratios in the total feed are 0.19, 0.98, and 3.07, respectively. The net result is a more contracted, volcano-shaped curve (see Figure 11) compared with the once-through case (see Figure 2). Therefore, the feed gas composition should be considered a crucial parameter in process development. Certainly, the superior heat management provided by liquid phase, slurry bubble column reactor-based syngas-to-DME processes gives one the flexibility to explore the feed gas composition as a way to optimize the productivity.

The above examples demonstrate that the integration between syngas generation and DME synthesis provides an opportunity to produce DME from syngas efficiently and at a high reactor throughput. This, in turn, should allow production of DME from syngas at a low cost. These advantages are achieved by adjusting the H_2:CO ratio in natural gas-derived syngas to fit the optimal operation of the DME reactor and by minimizing materials loss. The new process schemes also eliminate CO_2 emissions.

These process concepts provide a good basis for developing commercial packages. However, whether the higher productivity leads to lower DME production cost is a more complex issue. This depends on what additional cost has been introduced in the proposed process schemes. The integration-induced cost in the reformer part of the integration appears to be small. Carbon dioxide and H_2O recycle, used in the first three examples to enhance methane conversion and mitigate coke formation, may be a cost burden, but this recycle is a common feature of methane reforming, and therefore may not be a cost added by the integration.

The main added cost in the proposed process schemes is associated with CO_2 separation downstream of the DME reactor and CO_2 recycling to the methane reformer. Obtaining optimal DME production requires CO_2 removal from the DME reactor recycle. If not removed, CO_2 reduces the DME productivity by (1) diluting the reactor feed and (2) building up water in the reactor, as shown in Section 3.

However, CO_2 removal requires CO_2 separation from unconverted syngas and incurs additional production cost. The problem of carbon dioxide is not confined to the region where the optimal DME productivity is obtained (around 1:1). It is a more general problem, and our simulations show that CO_2 will always accumulate in the recycle loop unless the H_2:CO ratio in the total feed

to the reactor is very high (for example, 4:1). The effect of CO_2 separation and recycle on the economics of the process requires detailed engineering study. A qualitative discussion on this issue is given in the next section.

In summary, we have shown through a simple process configuration that the DME productivity and material utilization in a one step syngas-to-DME reactor with recycle is a very strong function of the feed gas composition. The optimum is obtained at a H_2:CO ratio of 1:1. While this condition and configuration provide optimal reactor performance, they produce CO_2 and require a feed gas having equal moles of H_2 and CO. Integrating DME production with syngas generation can solve this dilemma. This was shown by both conceptual process schemes and simulations under commercially relevant conditions using realistic reactors, kinetics and thermodynamics. As a result, the current study constitutes a good basis for developing commercial syngas-to-DME processes that provide optimal DME productivity and minimize emissions and material loss. Furthermore, all of these can be achieved using natural gas as the starting material.

5. Operating Regimes for Syngas-to-DME and Economic Implications

The last two sections demonstrate that the regime around a H_2:CO ratio of 1:1 provides the best productivity in a syngas-to-DME process. However, there are other cost factors in addition to reactor productivity that make the selection of operating regime a more complex issue. The current section discusses the trade-offs one must deal with in the syngas-to-DME process and the compromises affecting productivity that must be made. Efforts are also made to compare qualitatively the syngas-to-DME process with the two-step DME process, namely, syngas-to-methanol followed by methanol dehydration.

Figure 17 shows the enhancement in methanol equivalent productivity (MEP) of the syngas-to-DME process (STD) compared to the syngas-to-methanol process (STM). The comparison is made for two possible cases. In the first case, the productivity from STD at any H_2:CO ratio in the reactor feed is compared to that from STM at the same H_2:CO ratio. This corresponds to possible commercial situations where the composition of feed syngas is fixed, and one needs to decide whether STD or STM would yield the greater economic benefit. In the second case, the productivity of STD at any H_2:CO ratio in the reactor feed is compared with the productivity of STM at a H_2:CO ratio of 2. This is the case in which the syngas is derived from natural gas and the STM operates at its best feed composition (H_2:CO of 2), and therefore, highest productivity. Also plotted in Figure 17 are the exit CO_2 and H_2O concentrations from the STD process. They are related to the counter factors to be discussed below. All results in Figure 17 are from ASPEN simulations.

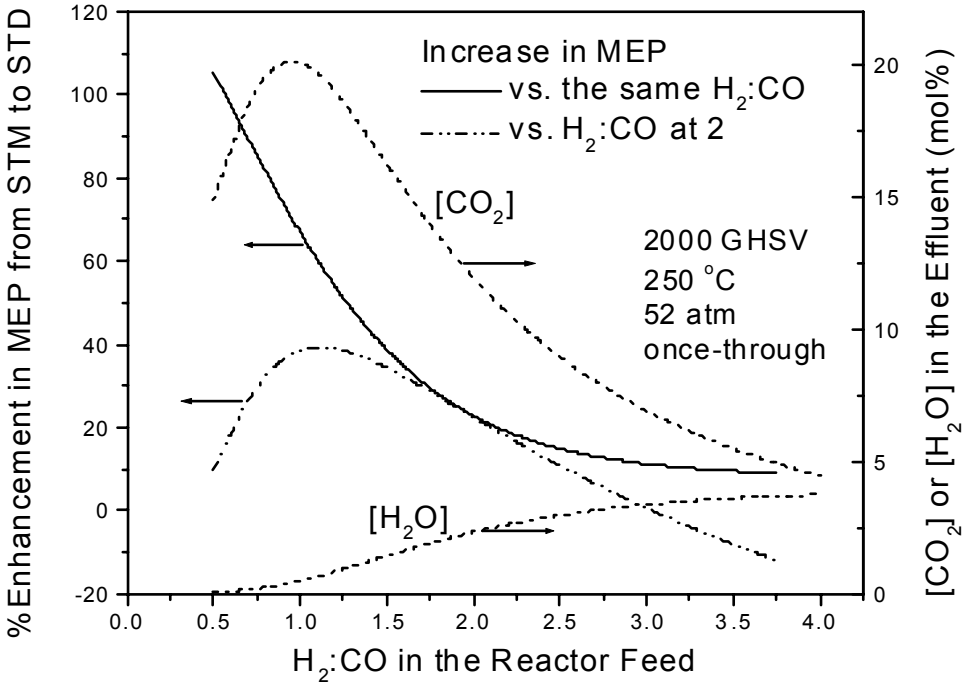

Figure 17: The trade-off between enhanced productivity and resulting CO_2 separation.

The productivity enhancement curves in Figure 17 are somehow proportional to the cost saving in the synthesis loop. This saving provides the very possibility for STD (one-step DME process) to be a more economic DME process than STM plus methanol dehydration (two-step DME process). Let us denote this saving as $\Delta_{synthesis}$. In general, greater enhancement is obtained when the feed gas moves from H_2-rich to CO-rich. This suggests that operating in the CO-rich regime (e.g., H_2:CO = 1) may make the STD process the most competitive..

Now let us look at the other parts of the one-step and two-step DME processes. The syngas generation cost is similar for the two processes and will not be discussed further. The backend part for the two-step process consists of methanol dehydration and separation between methanol and unconverted syngas, methanol and DME, and methanol and water. The methanol-syngas separation can be accomplished by simple condensation, and all other separations are routine processes that do not require high-pressure operation and refrigeration.

Since STD is not a commercial process yet, there is not a definitive backend configuration. However, it will inevitably consist of separation between DME/methanol and unconverted syngas, methanol and DME, and methanol and water. The cost of methanol-DME and methanol-water separation in STD is expected to be similar to that in the two-step process. Separation of DME/methanol from unconverted syngas in STD will be more costly than the separation of methanol from unconverted syngas in the two-step process due to the high volatility of DME. However, this difference may become small if one adds the cost of methanol dehydration in the two-step process. Therefore, the components in the backend part of the STD process we have covered thus far should approximately trade off with those in the backend of the two-step process.

However, if one chooses a STD operating regime (e.g., H_2:CO <3) where CO_2 will be formed and has to be separated in the backend, there will be a considerable cost increase . Refrigeration or chemical absorption must be used to remove CO_2 from unconverted syngas, and both are energy-intensive unit operations. Further added to the backend will be CO_2-DME separation, a costly operation that may also require refrigeration. In a word, if CO_2 becomes part of the backend, its cost will most likely be greater that that of the backend for the two-step process. Let us denote this CO_2-associated cost as $\mathbf{\Delta_{CO2}}$. Whether STD can be a more economic DME process than the two-step process depends on the trade-off between $\Delta_{synthesis}$ and Δ_{CO2}.

Figure 17 shows that the productivity enhancement curve and the [CO_2] curve change in the same direction as a function of H_2:CO ratio. This means that one has to answer the trade-off question no matter where one operates. For Case 1 (the same feed composition, the solid curve) in the CO-rich regime (H_2:CO < 1), $\Delta_{synthesis}$ is very large and the trade-off most likely will be positive. This is the case, and regime where STD has a clear advantage over the two-step process. Commercially, this would be a once-through process using syngas derived from coal, petro-coke, municipal wastes, biomass and other solid and liquid source materials.

The trade-off becomes less clear in Case 2 (natural gas-derived syngas, dashed curve). This is a case where STD is against the best feed and operating conditions for STM. The greatest $\Delta_{synthesis}$ (40%) is obtained if one operates STD around a H_2:CO ratio of 1:1. Section 4 has shown that this 1:1 feed can be obtained from natural gas-derived syngas through the integration between the DME synthesis loop and syngas generation unit. However, this is also the regime forming the greatest amount of CO_2. This not only makes Δ_{CO2} large, it also increases the cost for CO_2 recycle to the syngas generation unit. One can try to reduce Δ_{CO2} and CO_2 recycle cost by moving to a more H_2-rich regime with less CO_2 formation. However, this would be accompanied by a decrease in productivity. While it is not clear whether STD can be better than the 2-step process in Case 2, it is clear that one needs to develop optimized STD process schemes for STD to have a good chance. This would involve maximizing the reactor productivity and minimizing CO_2 handling cost.

There are other process options, but their advantages over STM plus methanol dehydration are also not clear. CO_2 formation can be suppressed by recycling CO_2 back to the reactor along with unconverted syngas. The net CO_2 formation can be significantly reduced and one needs only to separate a small amount of CO_2 in the product stream or may not need to do it at all. However, CO_2 will build up in the recycle loop, if H_2:CO is not extremely high (for example, >4), and the presence of a large amount of CO_2 will decrease the reactor productivity through dilution and the negative impact on the chemical synergy (see Section 3). Therefore, it ceases to be an option when the H_2:CO in the reactor feed is, say, less than 2.

Another way to avoid dealing with CO_2 is to operate STD at the very H_2-rich regime (H_2:CO > <5). Due to a high H_2 concentration, CO_2 formation becomes negligible. A patent has been issued for a STD process in this regime [20], although Figure 17 shows a negative $\Delta_{synthesis}$. It is very questionable how a STD process could be advantageous in this regime. Furthermore, water concentration is very high, as shown in Figure 17. High water concentration reportedly causes catalyst stability problems [21].

In summary, in the single-step STD process, the enhancement in reactor productivity is negatively compensated by the formation of CO_2. Since the costs associated with the reaction section and the separation section in such a process are in the same order of magnitude, it may need to be analyzed on a case-to-case basis whether the trade-off is sufficiently positive to justify using a single-step process over a two-step process. Any applications that demand high reactor productivity (e.g., once-through operation, CO-rich syngas) or/and allow lower CO_2 handling cost (e.g., high tolerance of CO_2 in the end use) will give a clear edge to the single-step process. Well-optimized process schemes and an active yet stable catalyst system that operates under the desired conditions will also tilt the balance.

REFERENCES

1. U.S. Department of Energy (1997). *Clean Coal Today* (26), 1.

2. Brown, D. M., Bhatt, B. L., Hsiung, T. H., Lewnard, J. J. and Waller, F. J. (1991) *Catalysis Today* **8**, 279.

3. Bhatt, B. L., Toseland, B. A., Peng, X. D., Heydorn, E. C., 17th Annual International Pittsburgh Coal Conference, Pittsburgh, PA, September, 11-15, 2000.

4. Fleisch, A. B., Gradassi, M. J., Masin, J. G., *Stud. Surf. Sci. Catal*. 107, 1997, 117.

5. Chen, Z. H., Niu Y. Q., Coal Conversion (Chinese) 19, 1996, 37.

6. Sills, R., Gas to Market Conference, San Francisco, October 11-13, 2000.

7. Brown, D. M., Tijm, P. J. A., Miller, W. R., Toseland, B. A. and Waller, F. A. (1998) *Proceedings, 12th International Symposium on Alcohol Fuels* (Beijing, P.R. China).

8. Huang, D., Kang, G., Zhang, S. and Wang, X. (1996) *Natural Gas Chemical Industry* **21**, 43.

9. Pop, Gr., Cherebetiu, T., Boeru, R., Ignatescu, Gh. and Albulescu, V. (1997) *Proceedings, The Research, Design and Construction of Refrigeration and Air Conditioning Equipment in Eastern European Countries* (Bucharest, Sept. 10-13, 1996) p.159.

10. Zahner, J. C. Conversion of Modified Synthesis Gas to Oxygenated Organic Chemicals. *U.S. Patent 4,011,275,* 1977.

11. Fujimoto, K., Asami, K., Shikada, T. and Tominaga, H. Selective Synthesis of Dimethyl Ether from Synthesis Gas. *Chem. Letters* **1984**, 2051.

12. Bharat, B., Topical Report prepared for DOE by Air Products and Chemicals, Contract No. DE-AC22-90PC89865, September 1992.

13. Tao, J., Niu, Y. and Chen, Z. (1991) *Natural Gas Chemical Industry* **16**, 17.

14. Gogate, M. R., Lee, S. and Kulik, C. J. Single-Stage, Liquid-Phase Dimethyl Ether Synthesis Process from Syngas. I: Dual Catalytic Activity and Process Feasibility. *Fuel Sci. Tech. Int'l.* **1991**, *9*, 653.

15. Hansen, J. B.; Joensen, F. High Conversion of Synthesis Gas into Oxygenates. In *Natural Gas Conversion*; Holmen et al. Eds.; Elsevier Science B. V.: Amsterdam, 1991; pp 457-467.

16. Ohno, Y., Shikada, T., Ogawa, T., Ono, M., Mizuguchi, M. and Fujimoto, K. (1997) *Prepr. Pap*. - *Am. Chem. Soc., Div. Fuel Chem.* **42,** 705.

17. Bercic, G. and Levec, J. (1992) *Ind. Eng. Chem. Res*. **31**, 1035.

18. Shikada, T.; Ohno, Y.; Ogawa. T.; Ono, M.; Mizuguchi, M.; Tomura, K.; Fujimoto, K. Direct Synthesis of Dimethyl Ether from Synthesis Gas. *Stud. Surf. Sci.* **1998**, *119*, 515-520.

19. Gunardson, H. *Industrial Gases in Petrochemical Processing*; Marcel Dekker, Inc.: New York, 1998.

20. Hansen, J. B., Joensen F, Voss, B., WO Patent 96/23755, 1996.

21. Basu, A., WO Patent 00/47874, 2000.